Supporting Information

Pharmaceutical Salts to Improve Diffusion Permeability of a BCS class III β-blocker Drug Atenolol

Daliya K. Shajan,[a] Noopur Pandey,[b] Animesh Ghosh,[b] Anubha Srivastava,[c] Palash Sanphui*,[a]

[a]Department of Chemistry, Faculty of Engineering and Technology, SRM Institute of Science and Technology, Kattankulathur, Tamil Nadu 603203, India. E-mail: palashi@srmist.edu.in

[b]Solid State Pharmaceutics Research Laboratory, Department of Pharmaceutical Sciences & Technology, Birla Institute of Technology, Mesra, Ranchi - 835215, Jharkhand, India

[c]Department of Physics, University of Lucknow, University Road, Lucknow 226007, Uttar Pradesh, India.

Table of contents

Table S1. Hydrogen bond geometry (Å, °)

	D–H···A	D-H/ Å	H···A/Å	D···A/Å	D-H···A/°	Symmetry code
ATL-FUM hydrate	N1–H1A···O4	0.86	2.04	2.8269(1)	151	x,3/2-y,1/2+z
	N1–H1B···O1	0.86	2.25	3.0165(1)	149	-x,-1/2+y,1/2-z
	N2–H2A···O4	0.90	1.83	2.7338(1)	179	1-x,1-y,-z
	N2–H2B···O3	0.90	1.96	2.8280(1)	160	1-x,1-y,-z
	O3–H3···O5	0.84	1.78	2.6224(1)	174	1-x,1-y,-z
	O6–H6A···O5	0.84	2.06	2.8942(1)	177	-
	O6–H6B···O1	0.87	2.01	2.8082	176	x,-1+y,z
	C4–H4···O5	0.92	2.52	3.3875(1)	155	x,1+y,z
ATLADP hydrate	N1–H1A···O4	0.86	2.23	3.0801(3)	170	1-x,1-y,-z
	N1–H1B···O3	0.86	2.17	2.9958(3)	162	-1+x,y,Z
	N2–H2A···O14	0.89	1.94	2.7738(2)	156	2-x,1/2+y,1/2-z
	N2–H2B···O15	0.89	1.90	2.7575(2)	162	-
	O3–H3···O13	0.82	1.85	2.6626(2)	173	--
	N3–H3A···O10	0.86	2.24	3.0802(3)	164	2-x,1-y,-z
	N3–H3B···O9	0.86	2.18	2.9943(3)	158	-
	N4–H4A···O20	0.89	1.94	2.7920(2)	160	1+x,y,z
	N4–H4B···O17	0.89	1.87	2.7428(2)	168	-
	N5–H5A···O6	0.86	2.14	2.9633(3)	160	2-x,1-y,-z
	N5–H5B···O1	0.86	2.04	2.8829(3)	168	-
	O6–H6···O18	0.82	1.80	2.6202(2)	173	1+x,y,z
	N6–H6A···O13	0.89	1.90	2.7569(2)	162	2-x,1/2+y,1/2-
	N6–H6B···O16	0.89	1.95	2.7843(2)	156	2-x,1/2+y,1/2-
	N7–H7A···O4	0.86	2.15	2.9685(3)	160	1-x,2-y,-z
	N7–H7B···O12	0.86	2.02	2.8506(3)	163	-1+x,y,z
	N8–H8A···O18	0.89	1.89	2.7617(2)	168	1-x,1/2+y,1/2-
	N8–H8B···O19	0.89	1.90	2.7548(2)	161	2-x,1/2+y,1/2-
	O9–H9···O15	0.82	1.82	2.6339(2)	172	2-x,1/2+y,1/2-
	O12–H12A···O20	0.82	1.90	2.7178(2)	176	2-x,1/2+y,1/2-
	O21–H21A···O14	0.85	2.06	2.7595(2)	139	-
	O21–H21B···O24	0.85	1.96	2.7762(2)	161	1+x,y,z
	O22–H22A···O22	0.85	1.93	2.7782(2)	175	2-x,-1/2+y,1/2
	O22–H22B···O24	0.85	1.89	2.7384(2)	172	-
	O23–H23C···O21	0.85	2.07	2.7722(2)	140	-
	O24–H24A···O17	0.85	2.00	2.7838(2)	154	-
	O24–H24B···O23	0.85	1.89	2.7340(2)	170	-

Table S2. Calculation of Distribution Coefficients of ATL and its salts

Salts	C_w (mg/mL)	C_0 (mg/mL)	C_E (mg/mL)	$C_{initial}$ -C_E (mg/mL)	Log (C_0/C_w)	Log ($C_{initial}$-C_E)/C_E
ATL	1.035	0.3442	0.9041	0.1309	-0.47	-0.83
ATL-ADP	0.8869	0.3945	0.6590	0.2279	-0.351	-0.461
ATL-FUM	0.8150	0.5426	0.6647	0.1503	-0.176	-0.645
ATL-GLU	0.8084	0.4813	0.5646	0.2438	-0.22	-0.364
ATL-MAL	0.7833	0.3817	0.4954	0.2879	-0.312	-0.23
ATL-OXA	0.7786	0.4165	0.4915	0.2865	-0.271	-0.234
ATL-PIM	0.7291	0.4134	0.4734	0.2557	-0.251	-0.267

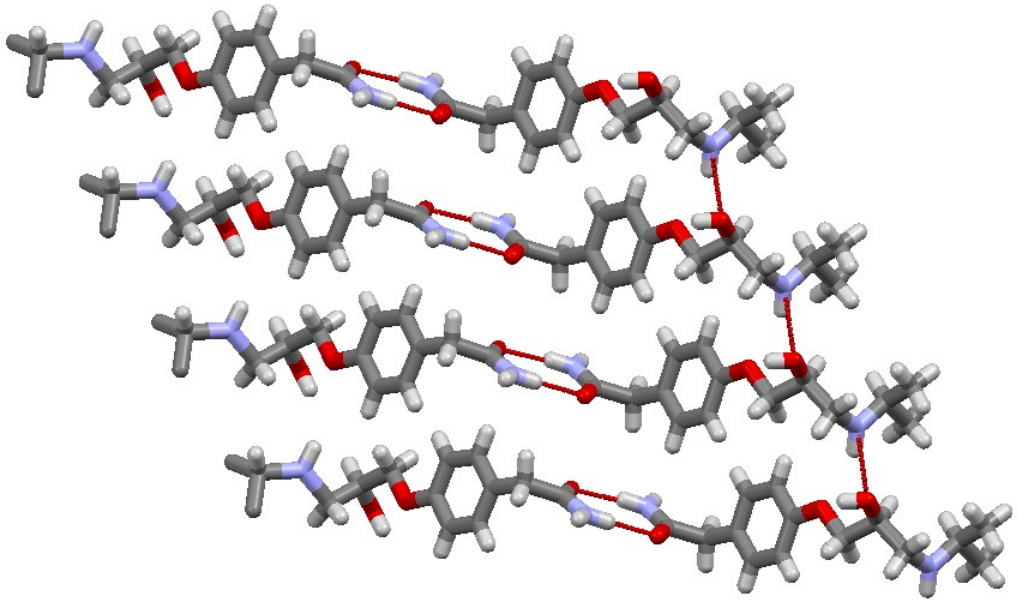

(a)

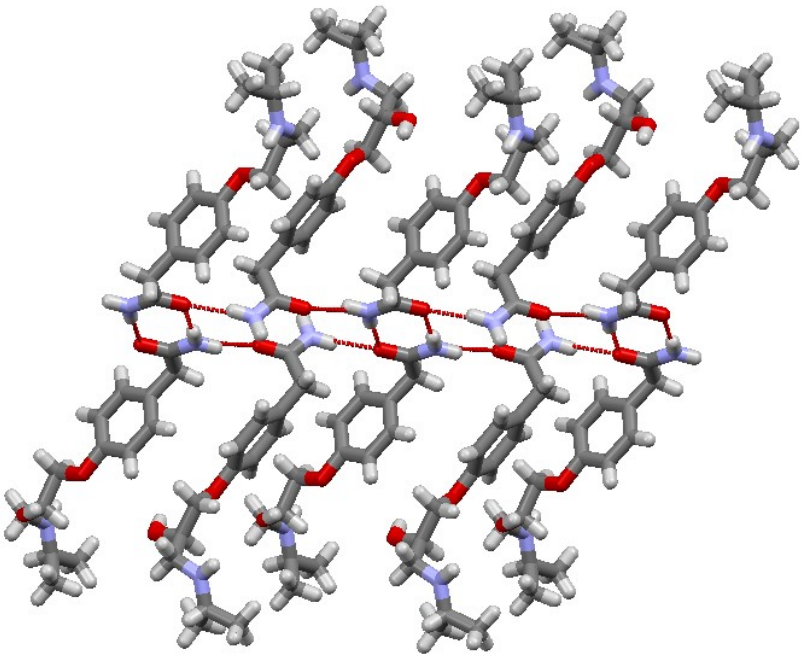

(b)

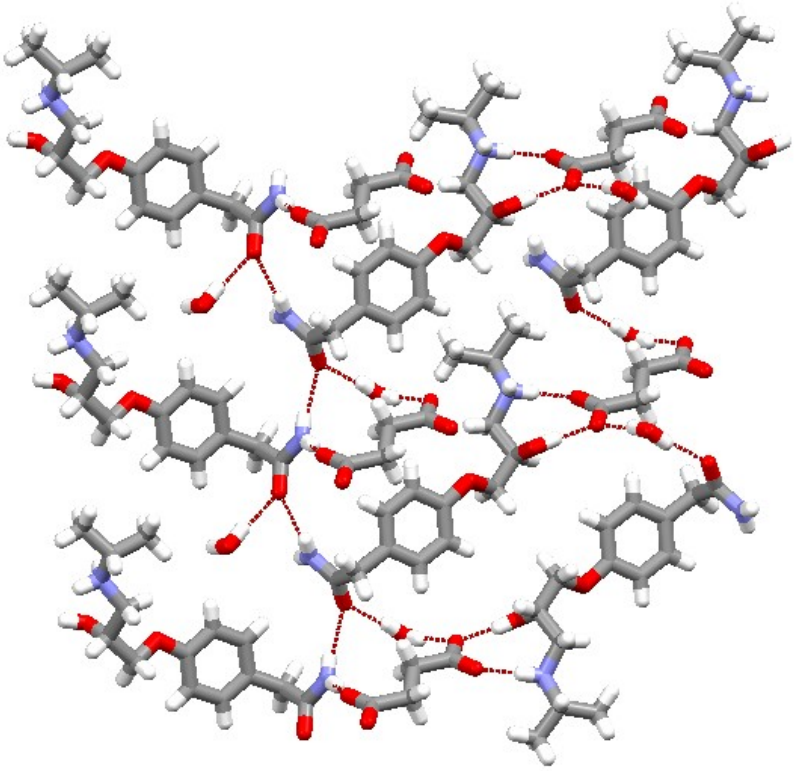

(c)

Figure S1. Hydrogen bonded amide dimer in a) S-ATL and b) RS ATL. c) ATL-succninate salt hydrate represents proton transfer from succinic acid to ATL, while amide fractions involved in catemer hydrogen bonds.

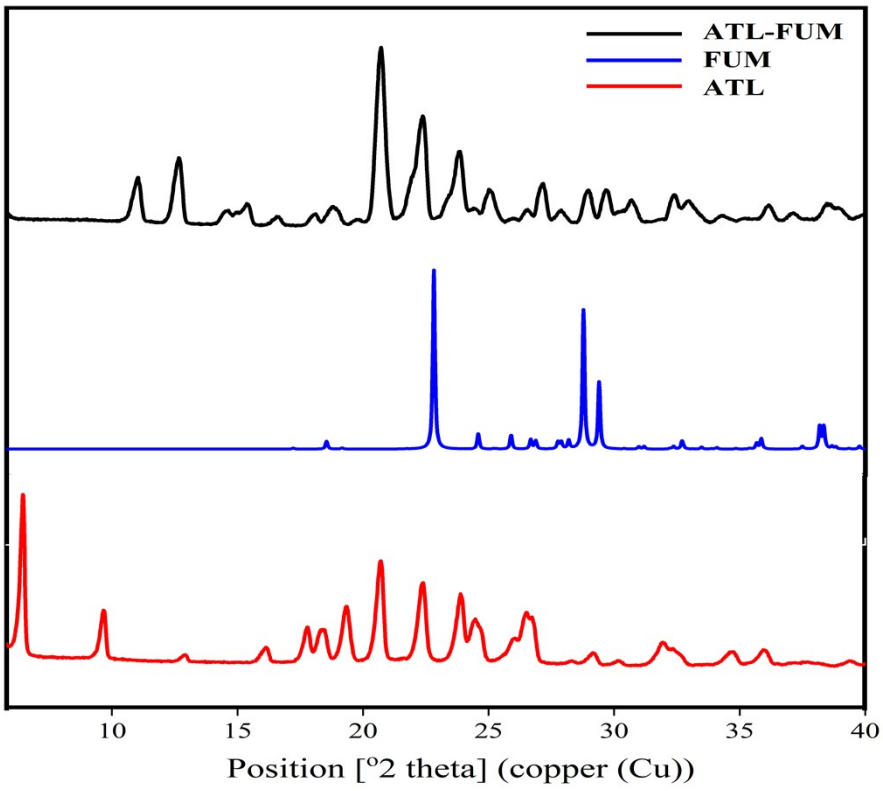
ATL-FUM
FUM
ATL
10
15
20
25
30
35
40
Position [°2 theta] (copper (Cu))

(a)

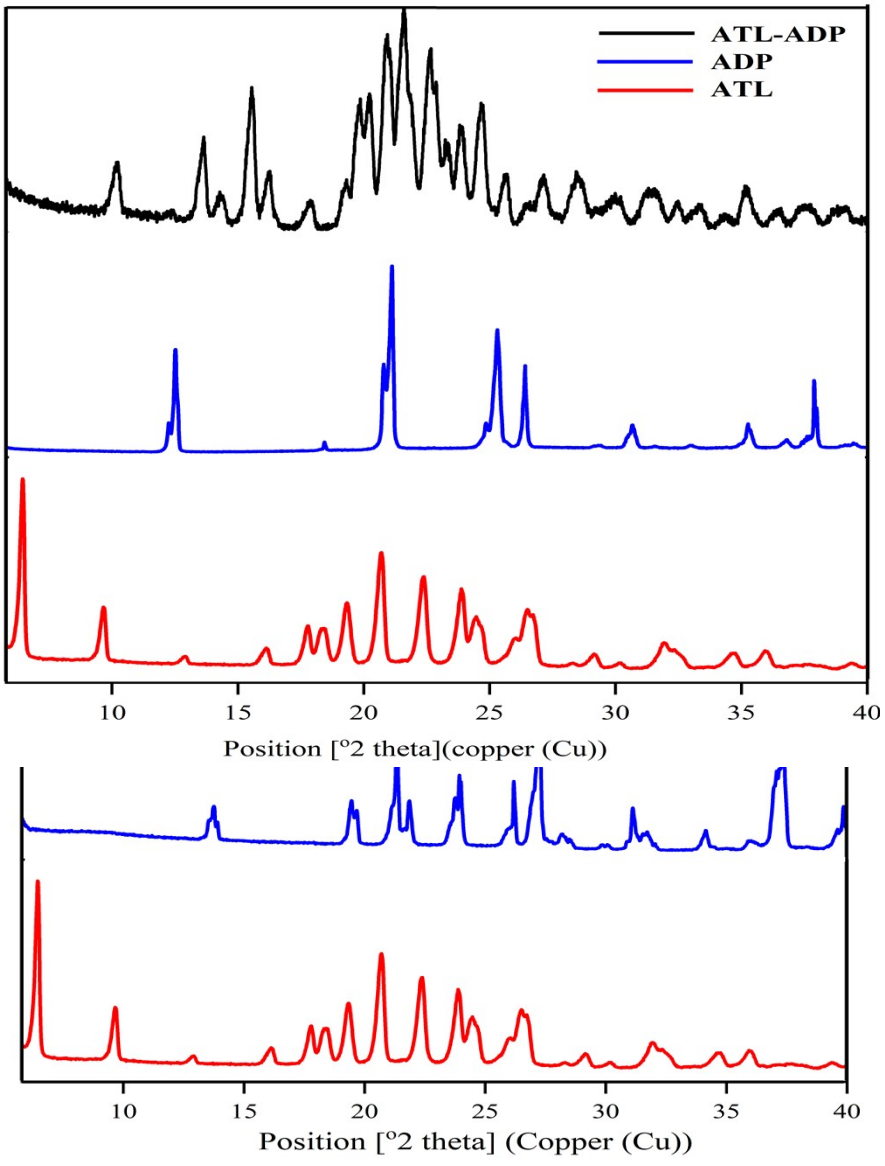
ATL-ADP
ADP
ATL
10
15
20
25
30
35
40
Position [°2 theta](copper (Cu))
10
15
20
25
30
35
40
Position [°2 theta] (Copper (Cu))

(c)

(c)

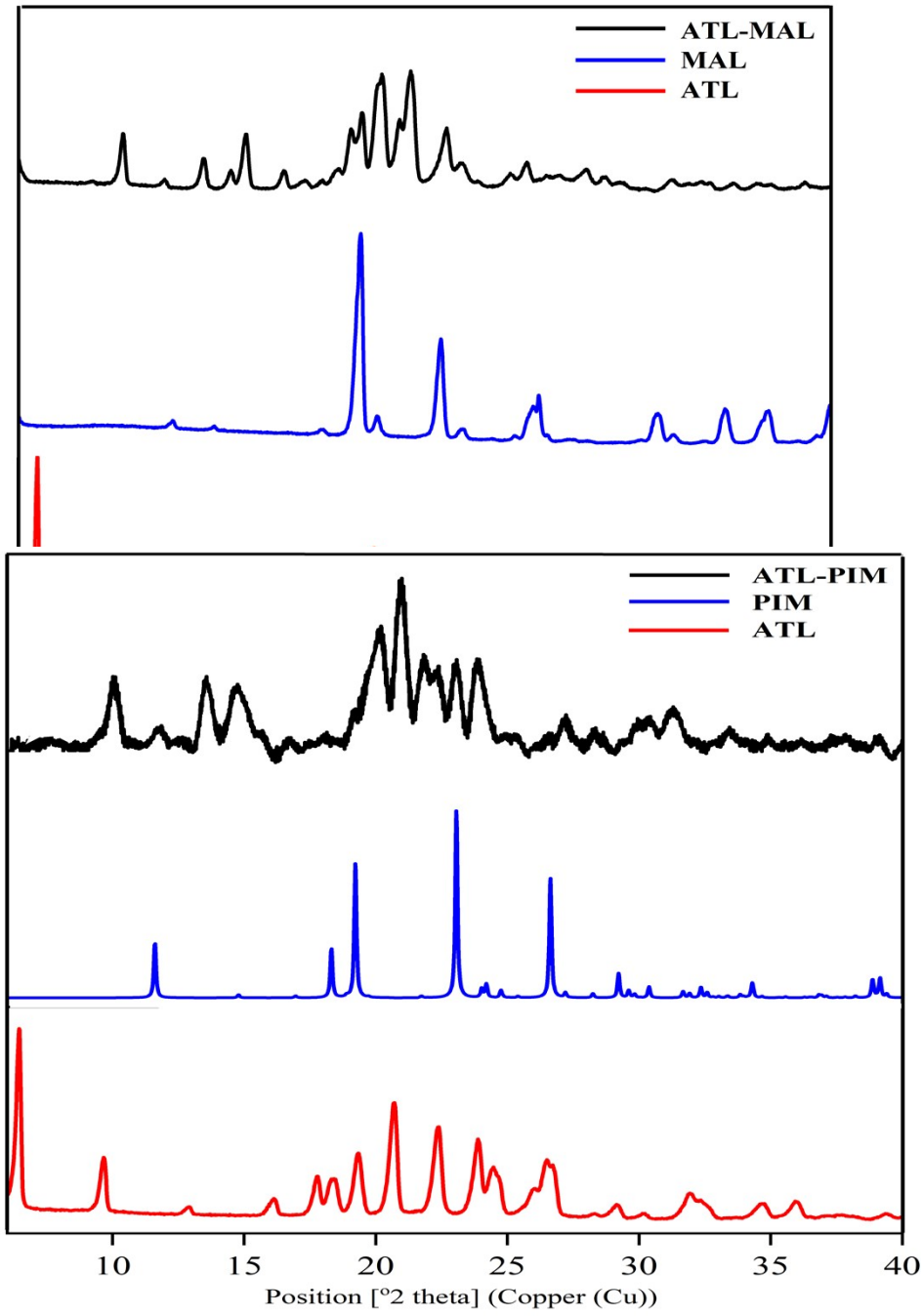
ATL-MAL
MAL
ATL
ATL-PIM
PIM
ATL
10
15
20
25
30
35
40
Position [°2 theta] (Copper (Cu))

(e)

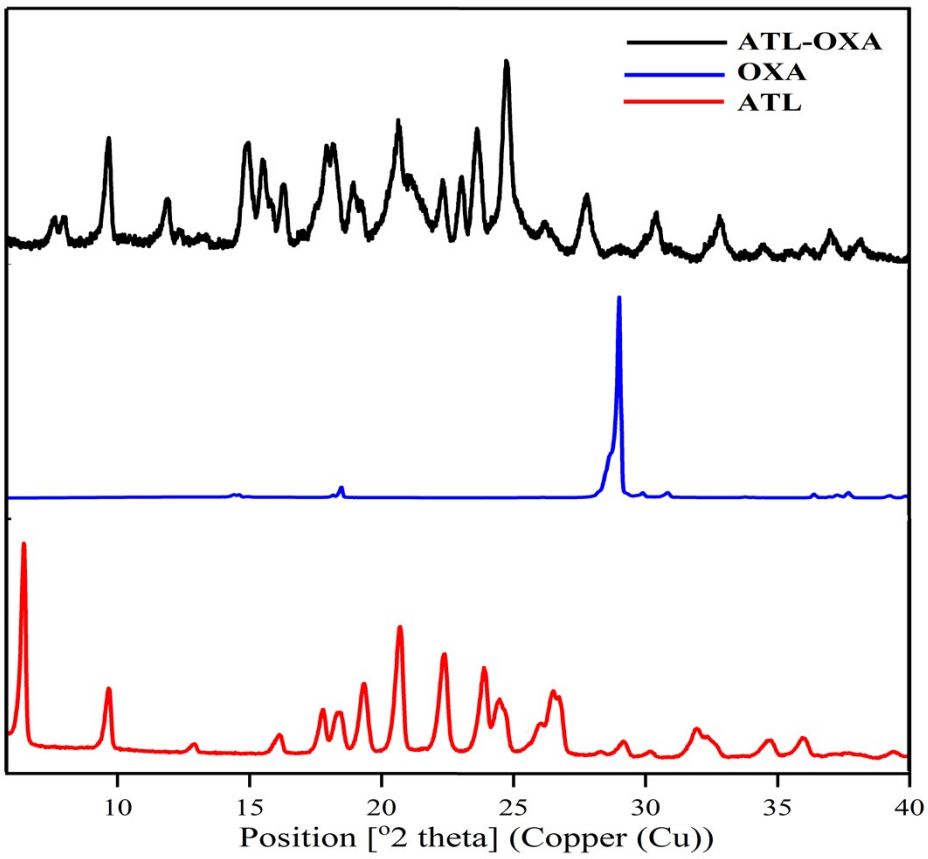

(f)

Figure S2. PXRD comparison of (a-f) ATL salts with that of ATL and salt former confirm their distinct phase

(a)

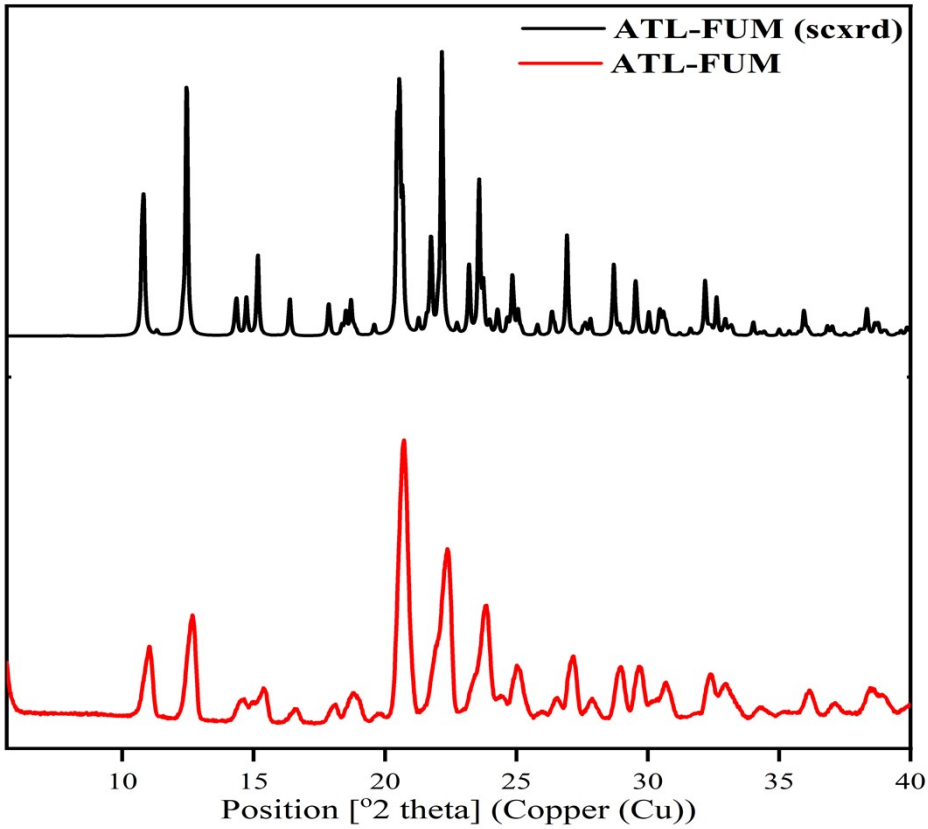
ATL-FUM (scxrd)
ATL-FUM
10
15
20
25
30
35
40
Position [°2 theta] (Copper (Cu))

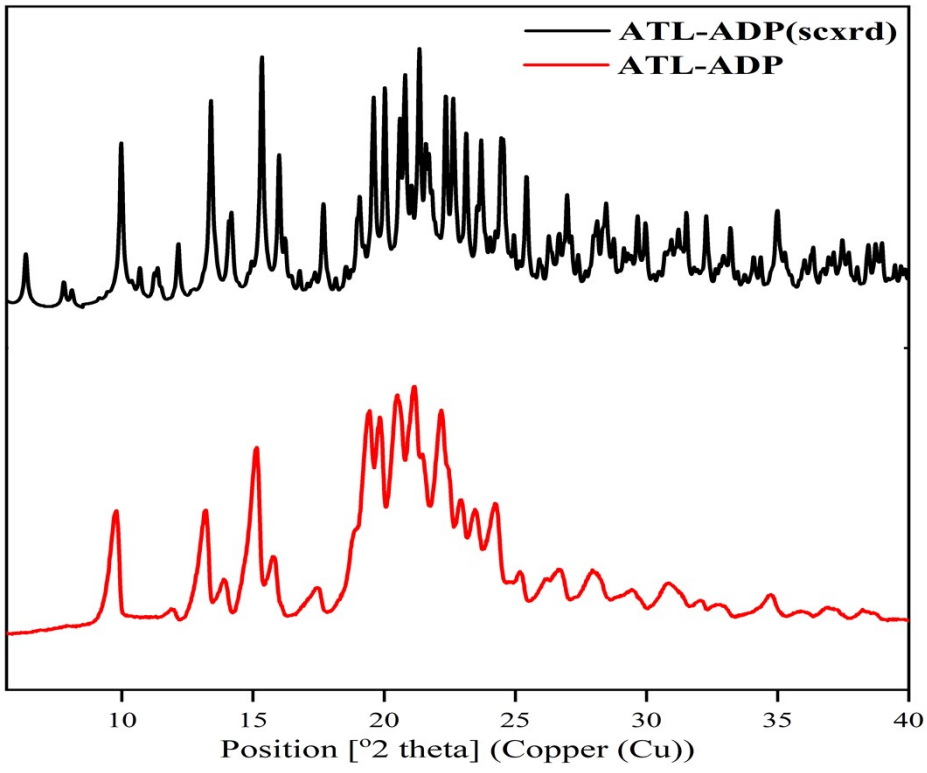
ATL-ADP(scxrd)
ATL-ADP
10
15
20
25
30
35
40
Position [°2 theta] (Copper (Cu))

(b)

Figure S3. Comparison of PXRD pattern of a) ATL-FUM, b) ATL-ADP with the calculated X-ray pattern from their crystal structures confirmed purity of the bulk phase. Note, slight deviation of ATL-ADP hydrate in the XRD patterns compared to its crystal structure pattern indicates instability of the phase.

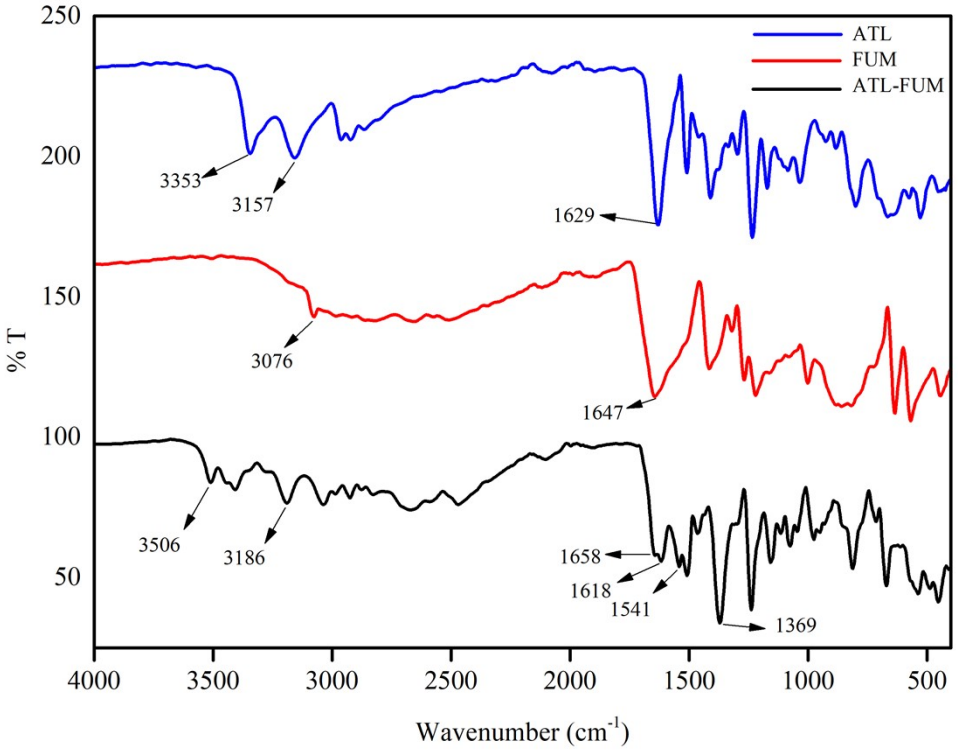

(a)

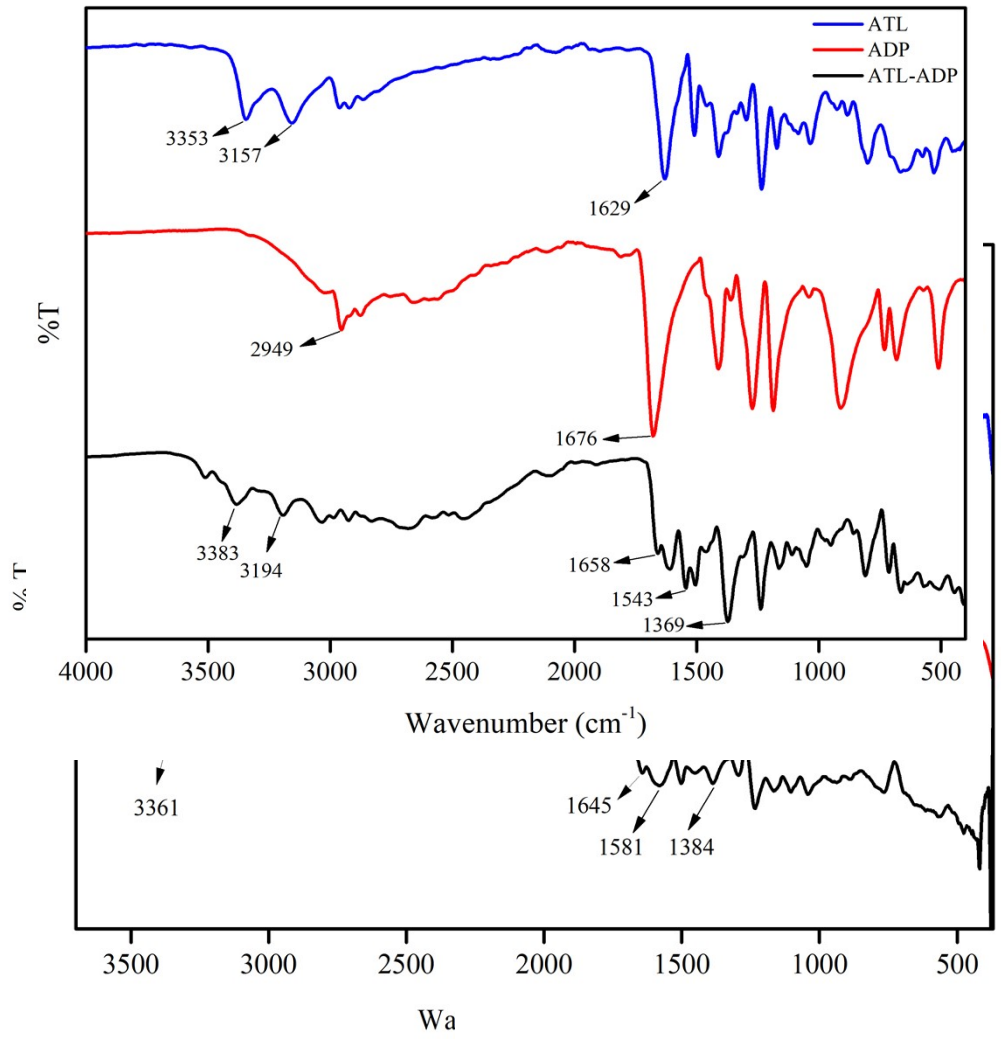

(c)

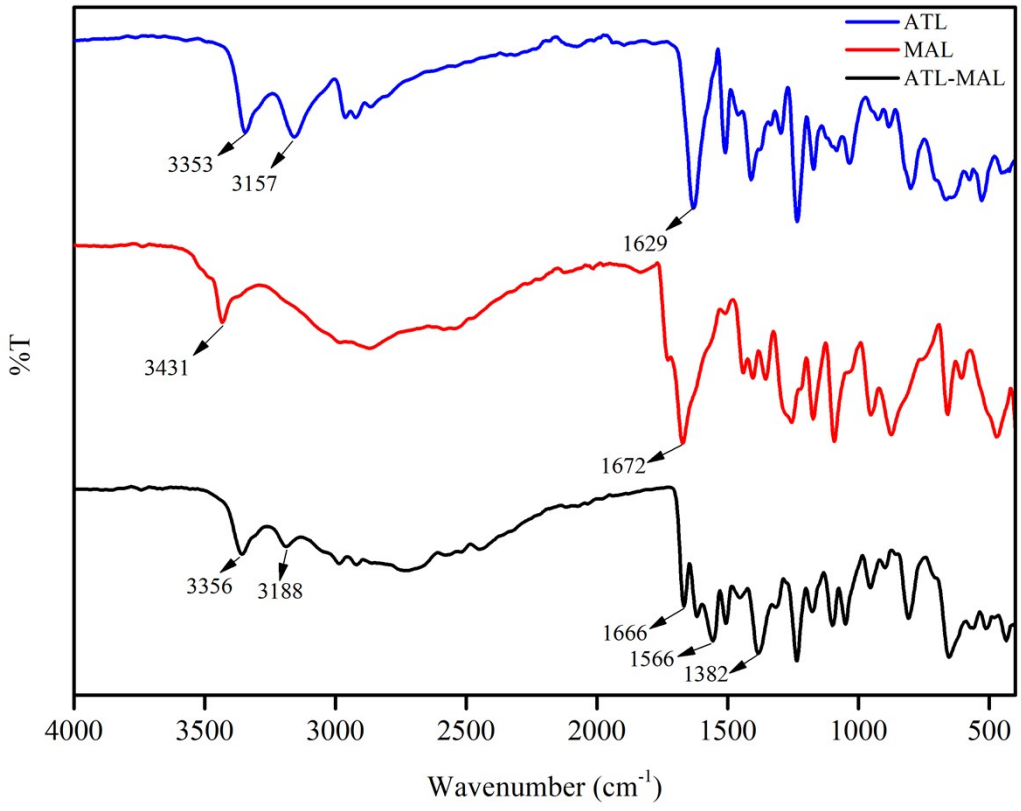
ATL
MAL
ATL-MAL
3353
3157
1629
3431
1672
3356
3188
1666
1566
1382
%T
4000
3500
3000
2500
2000
1500
1000
500
Wavenumber (cm-1)

(d)

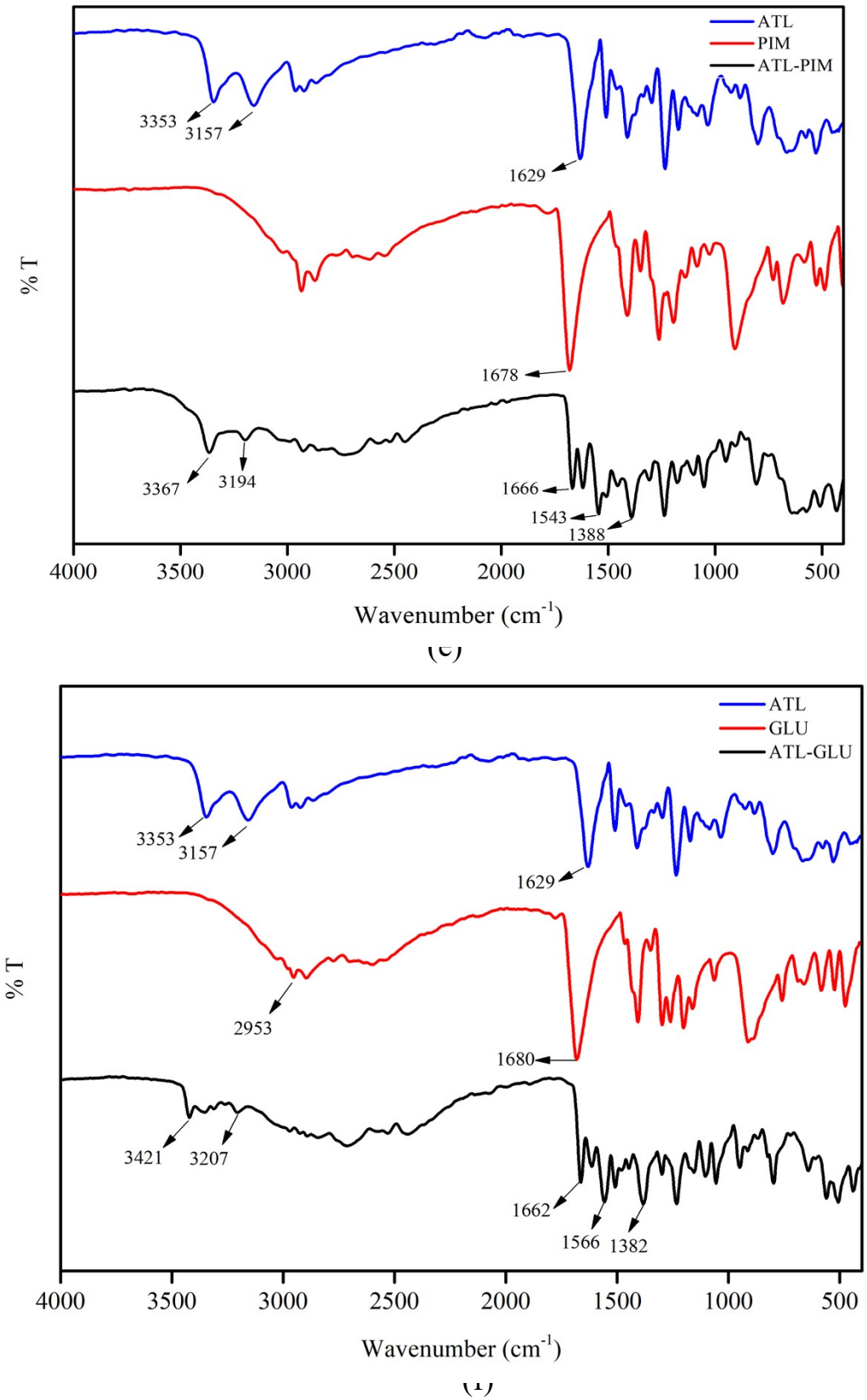

Figure S4. Vibrational frequencies comparison of ATL salts with ATL and salt formers (a-f).

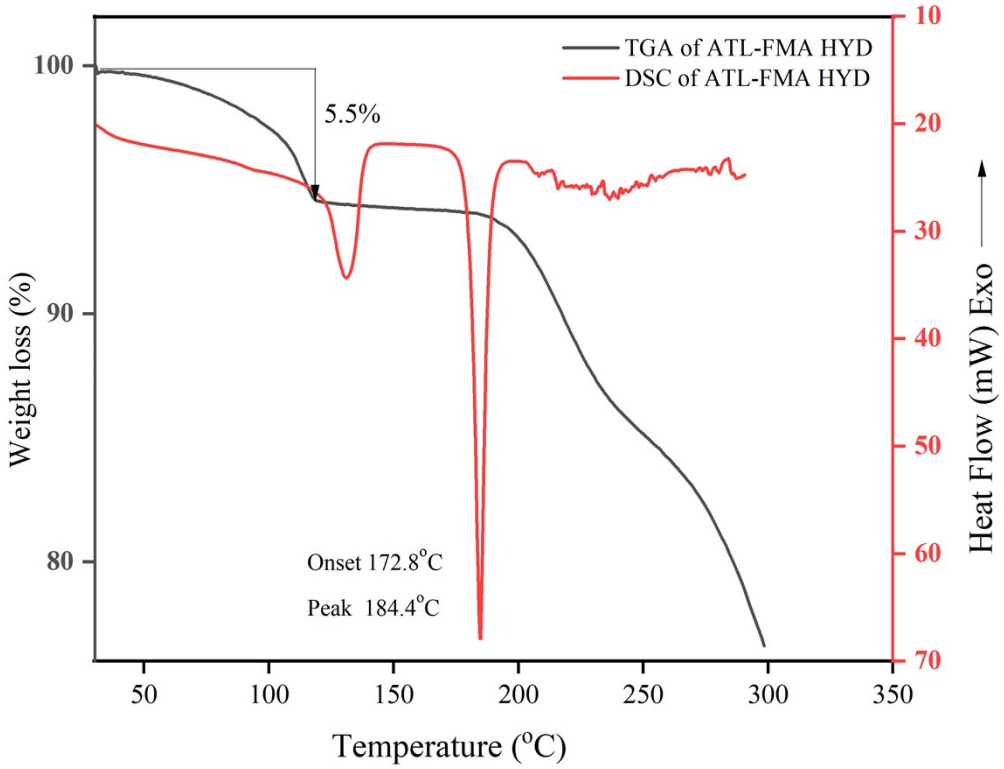
TGA of ATL-FMA HYD
DSC of ATL-FMA HYD
5.5%
Onset 172.8°C
Peak 184.4°C
Weight loss (%)
Heat Flow (mW) Exo
Temperature (°C)

(a)

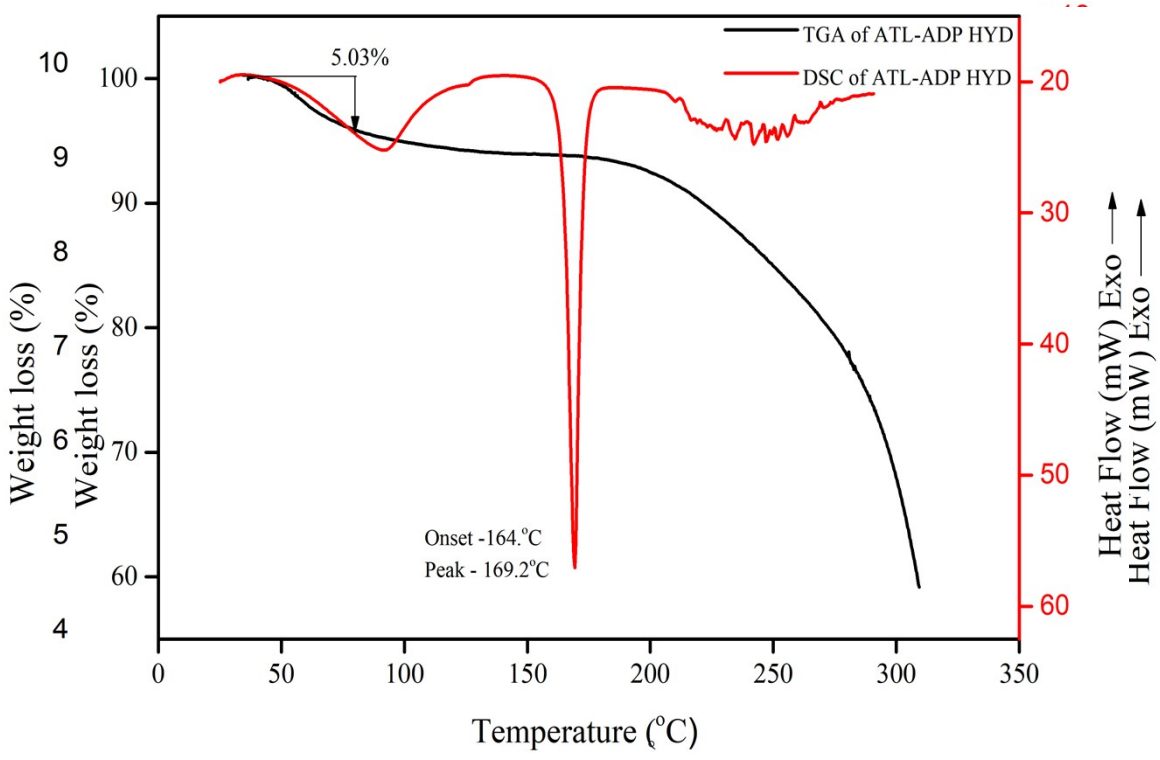
TGA of ATL-ADP HYD
DSC of ATL-ADP HYD
5.03%
Onset -164.°C
Peak - 169.2°C
Weight loss (%)
Heat Flow (mW) Exo
Temperature (°C)

(b)

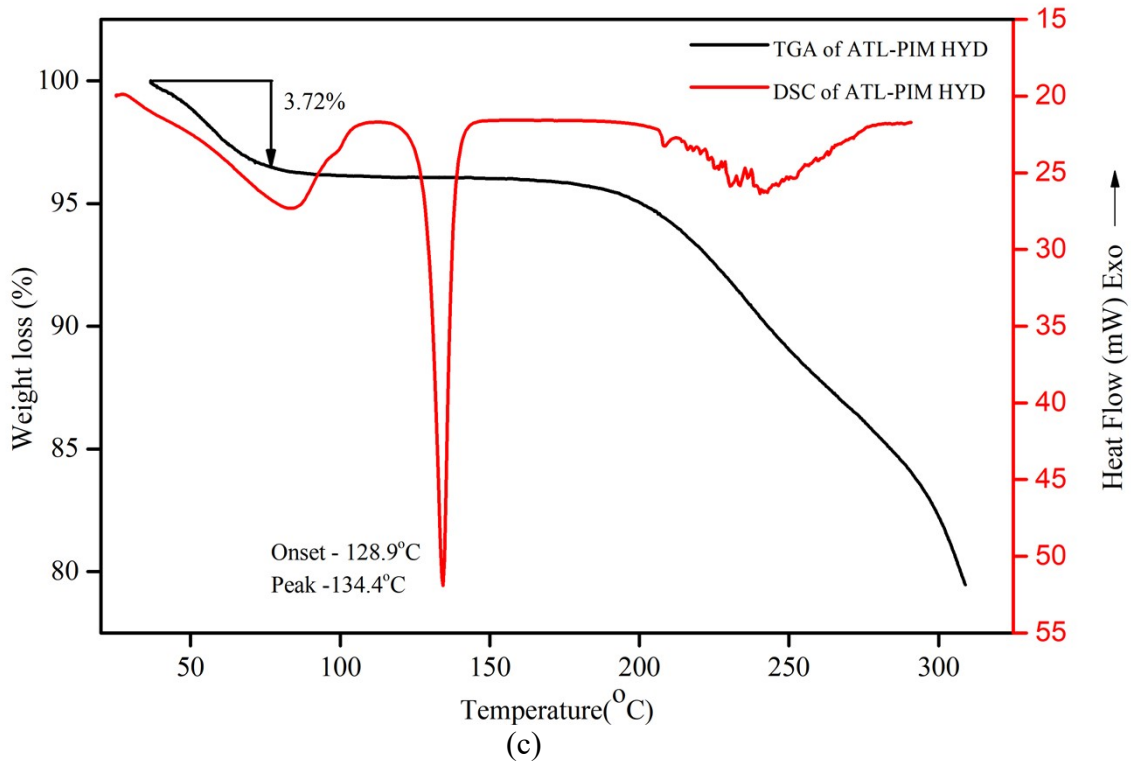

(d)

Figure S5. DSC -TGA thermograms of a) ATL-FUM, b) ATL-ADP, c) ATL-OXA, d) ATL-PIM salt hydrates.

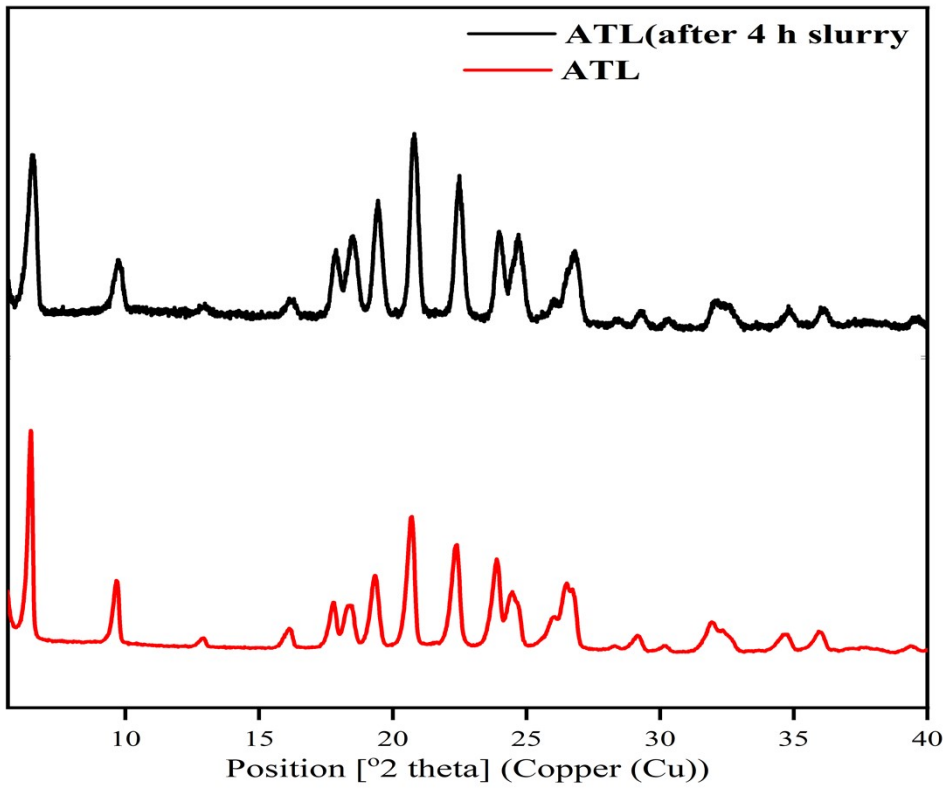

(a)

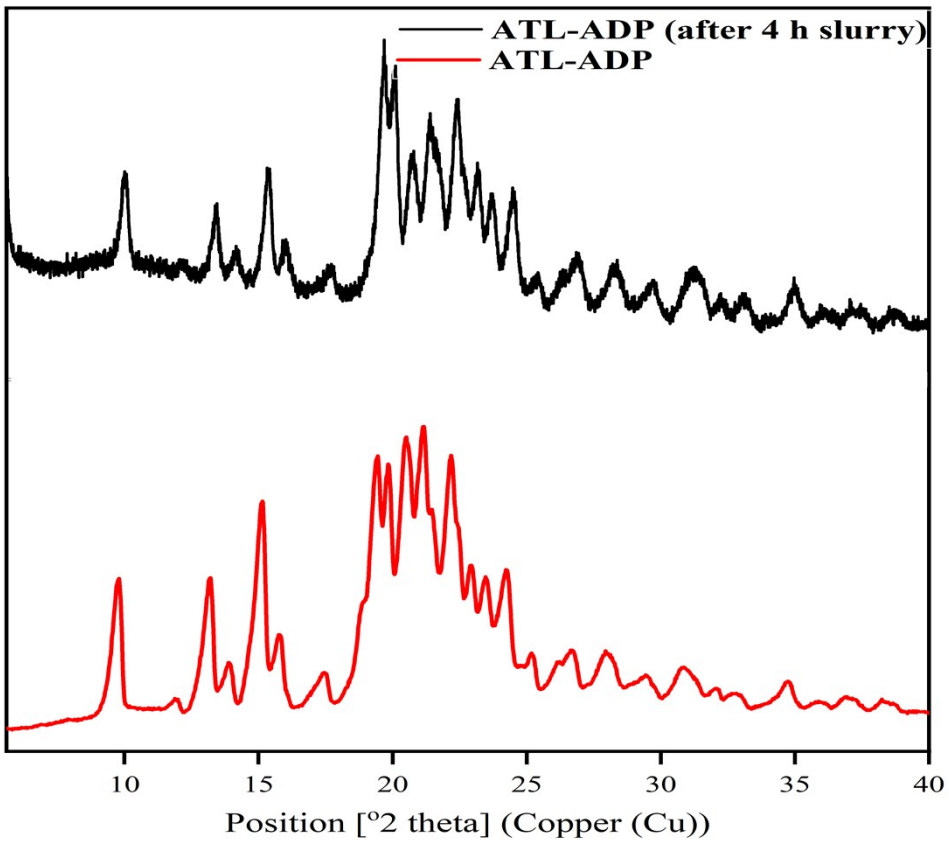
ATL-ADP (after 4 h slurry)
ATL-ADP
10
15
20
25
30
35
40
Position [°2 theta] (Copper (Cu))

(b)

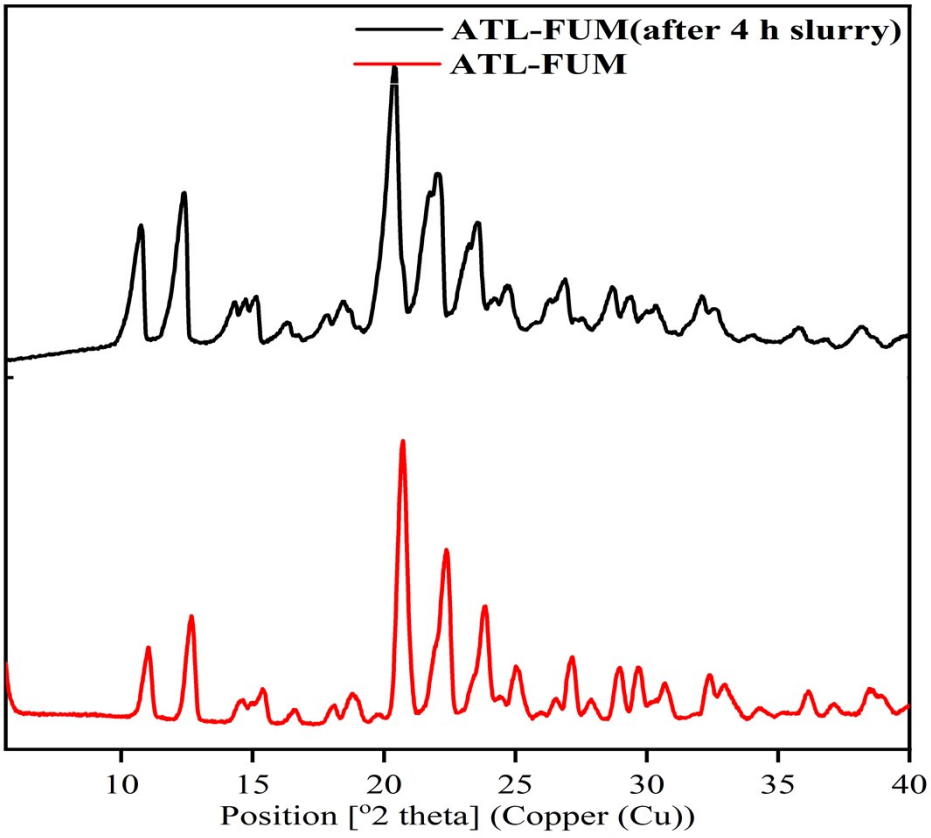
ATL-FUM(after 4 h slurry)
ATL-FUM
10
15
20
25
30
35
40
Position [°2 theta] (Copper (Cu))

(c)

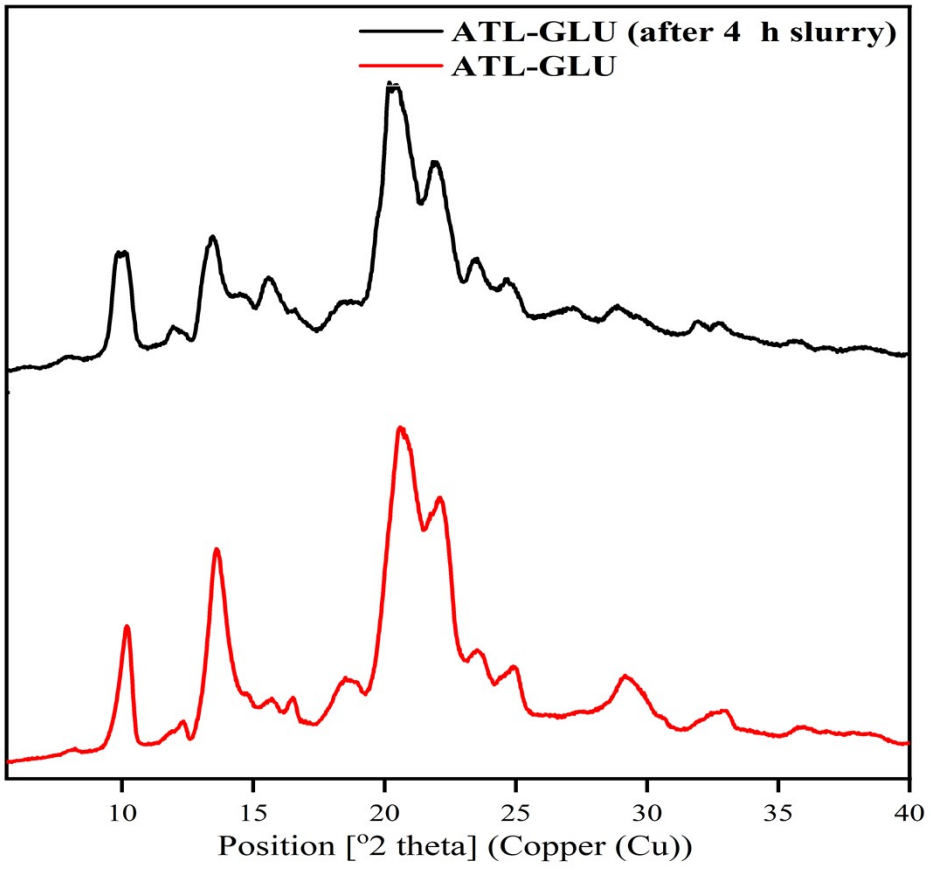
ATL-GLU (after 4 h slurry)
ATL-GLU
10
15
20
25
30
35
40
Position [°2 theta] (Copper (Cu))

(d)

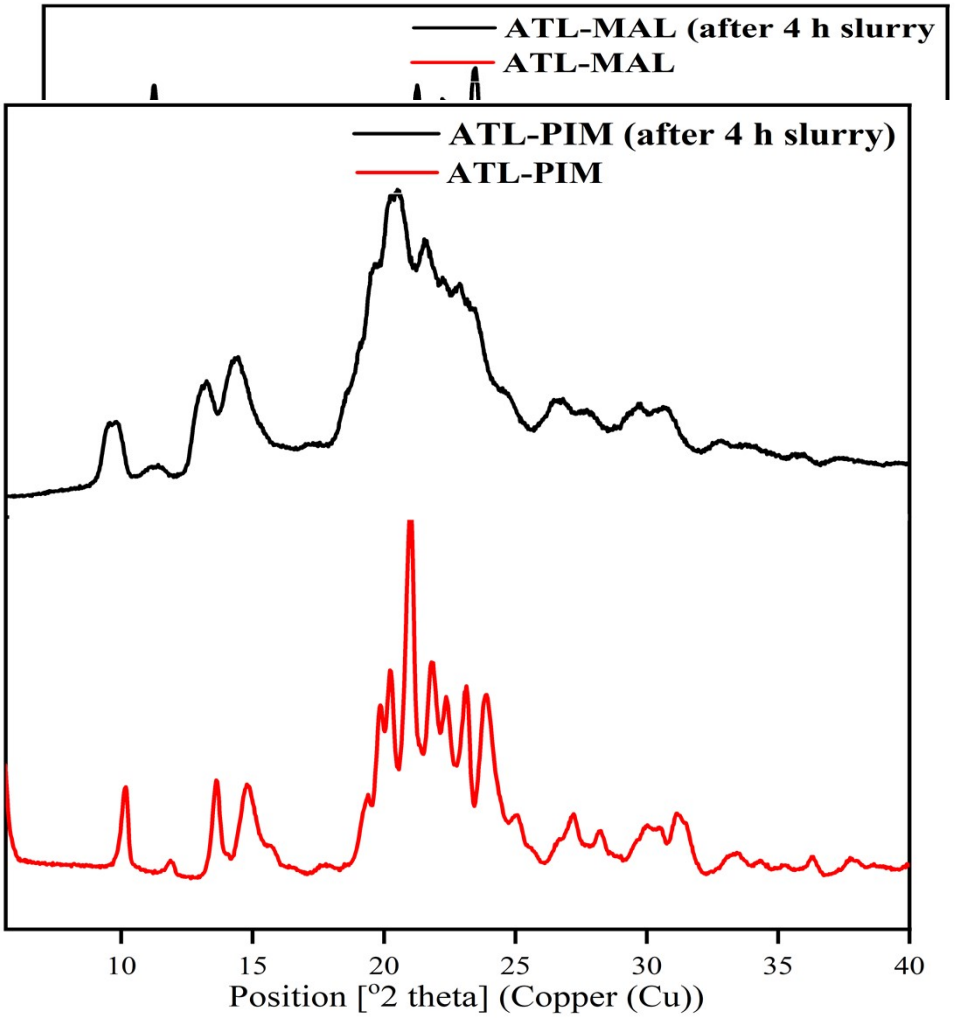

(g)

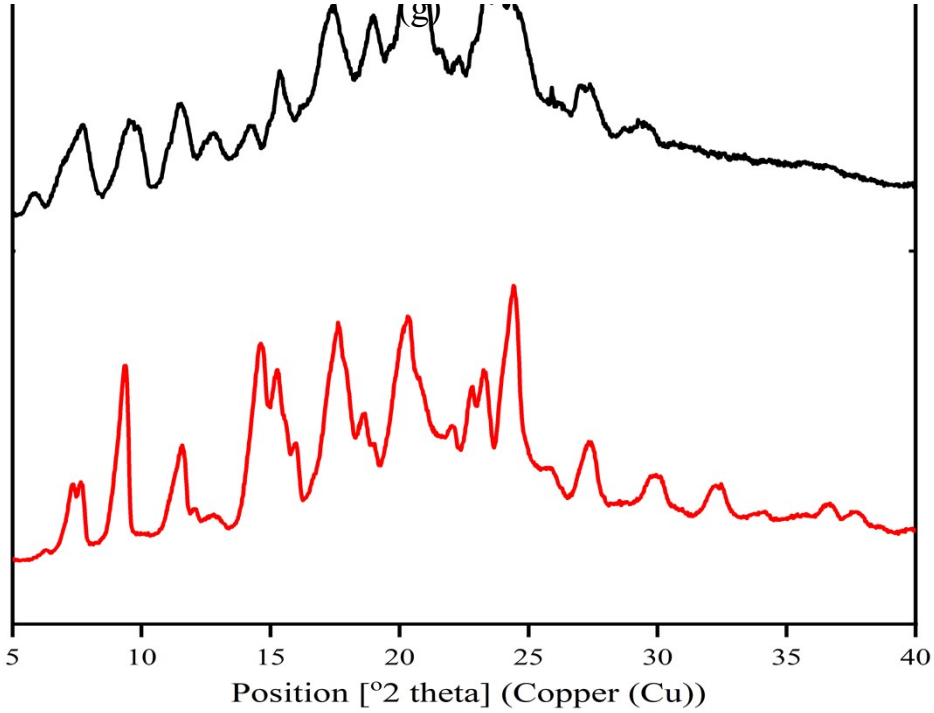

(f)

Figure S6. PXRD

comparison of ATL salts after solubility experimrnt confirmed that except ATL-OXA salt, others were stable in the aquoeus phase (a-g).

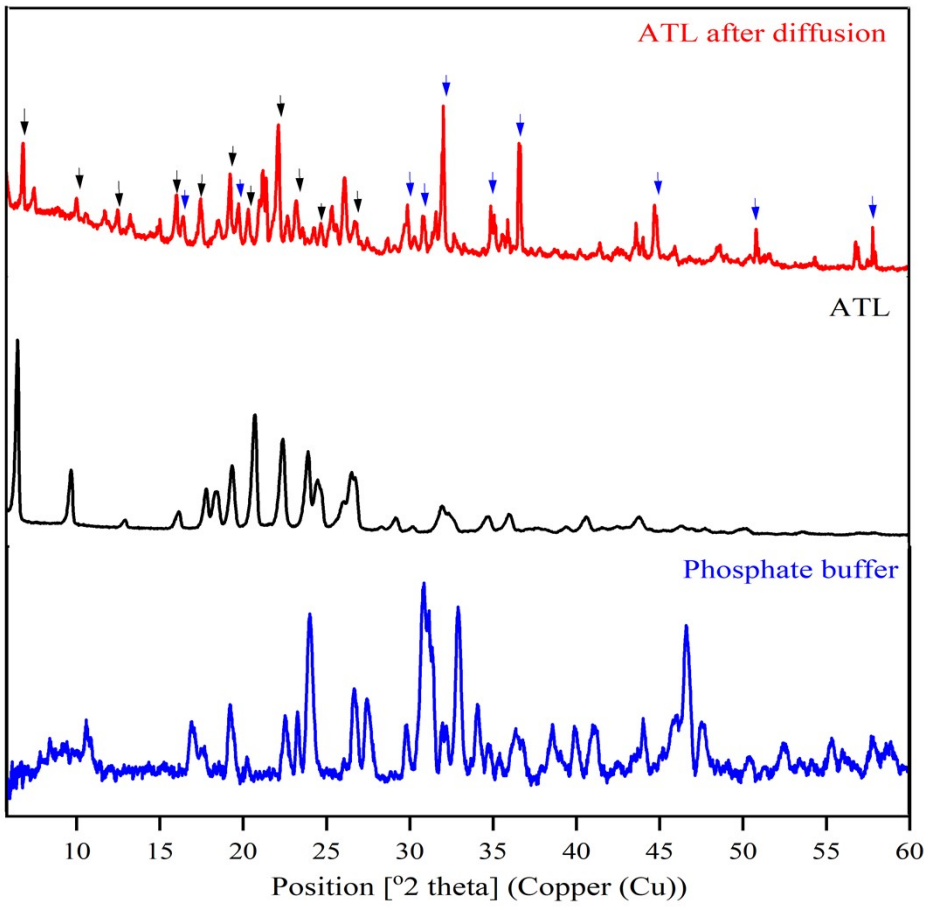

(a)

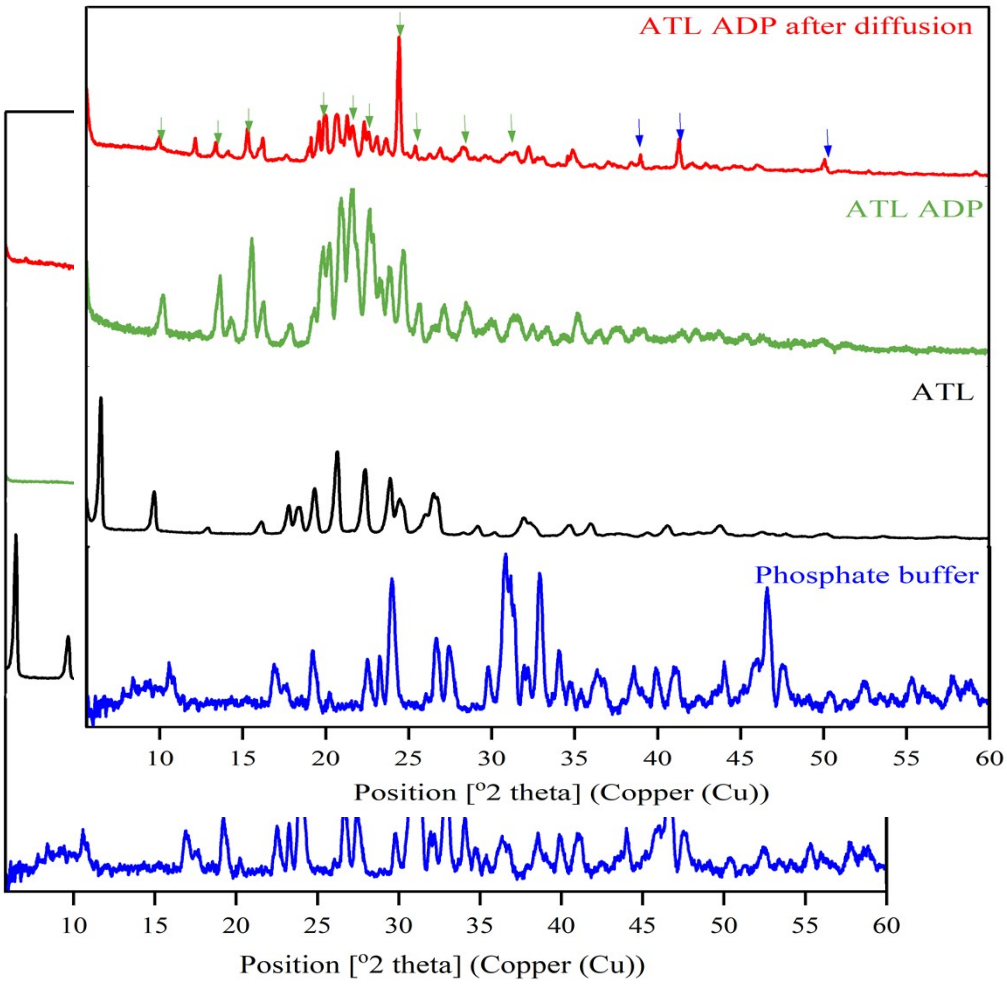

(c)

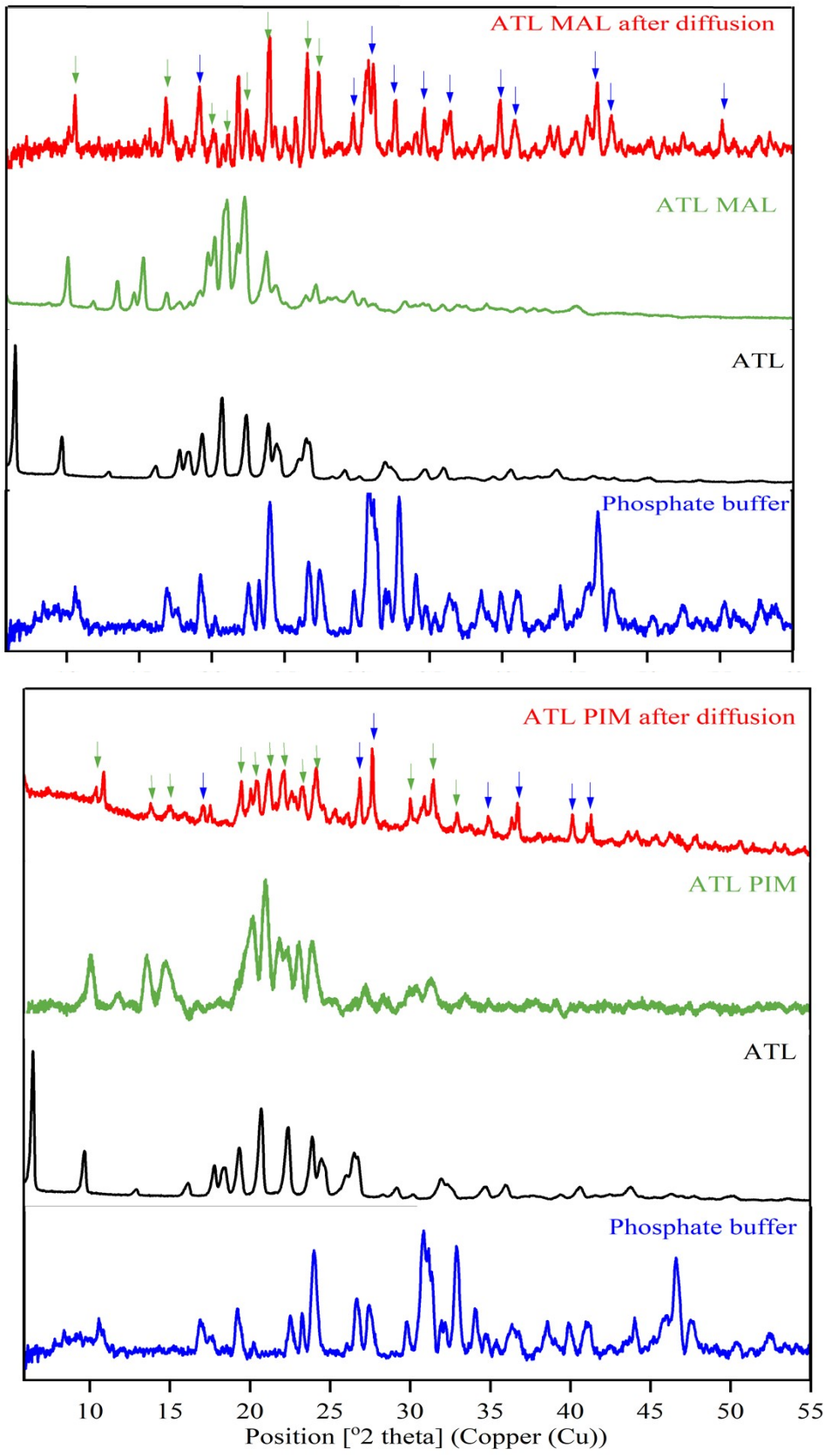
ATL MAL after diffusion
ATL MAL
ATL
Phosphate buffer
ATL PIM after diffusion
ATL PIM
ATL
Phosphate buffer
10
15
20
25
30
35
40
45
50
55
Position [°2 theta] (Copper (Cu))

(e)

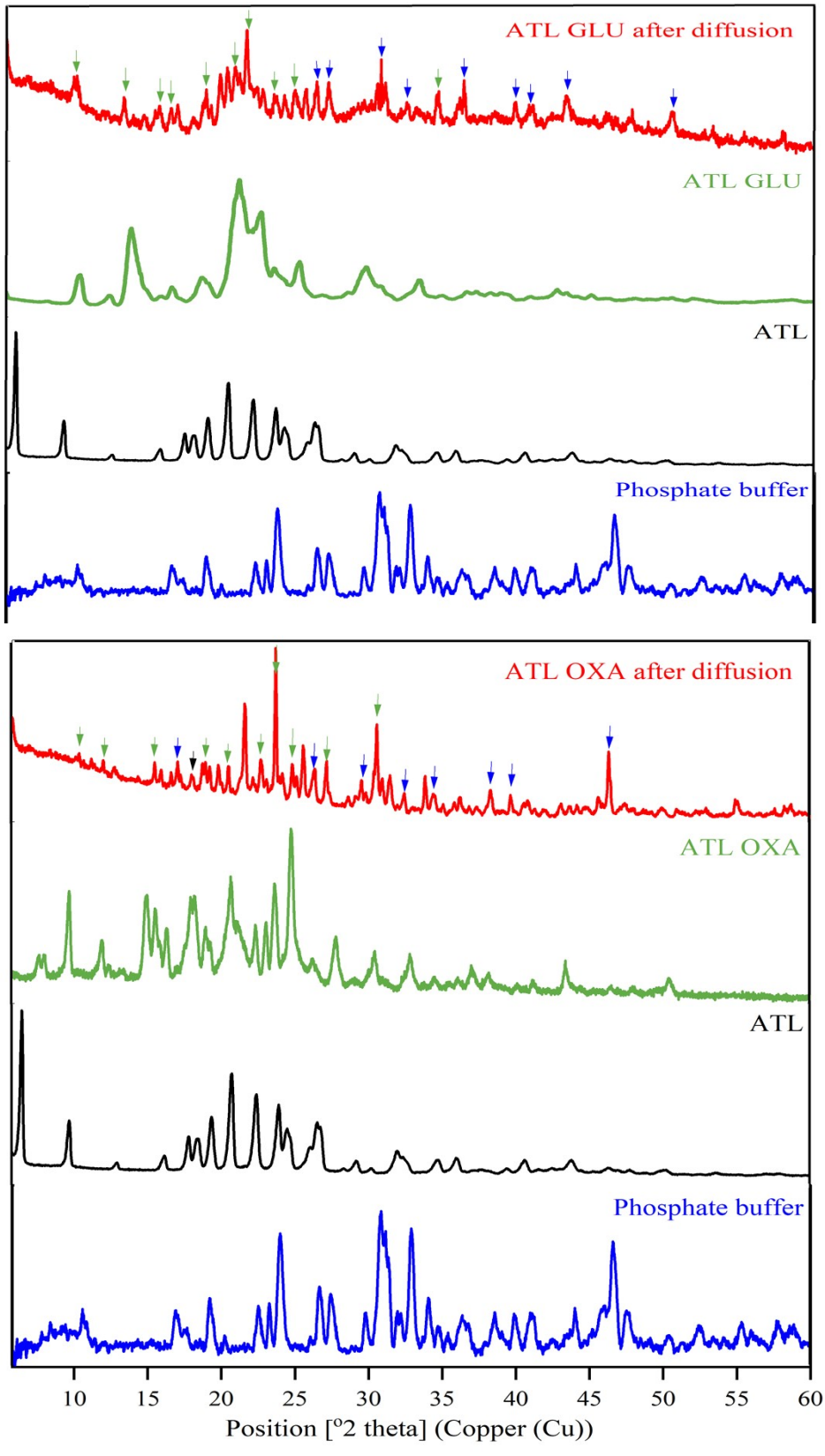
ATL GLU after diffusion
ATL GLU
ATL
Phosphate buffer
ATL OXA after diffusion
ATL OXA
ATL
Phosphate buffer
10
15
20
25
30
35
40
45
50
55
60
Position [°2 theta] (Copper (Cu))

(g)

Figure S7. PXRD comparison of ATL and its salts (a-g) after 6h diffusion experiment. Note, additional diffraction peaks correspond to the phosphate buffer salts which appear along with the native drug.(green arrow corresponds to the salt peaks and blue arrow corresponds to the buffer peaks)

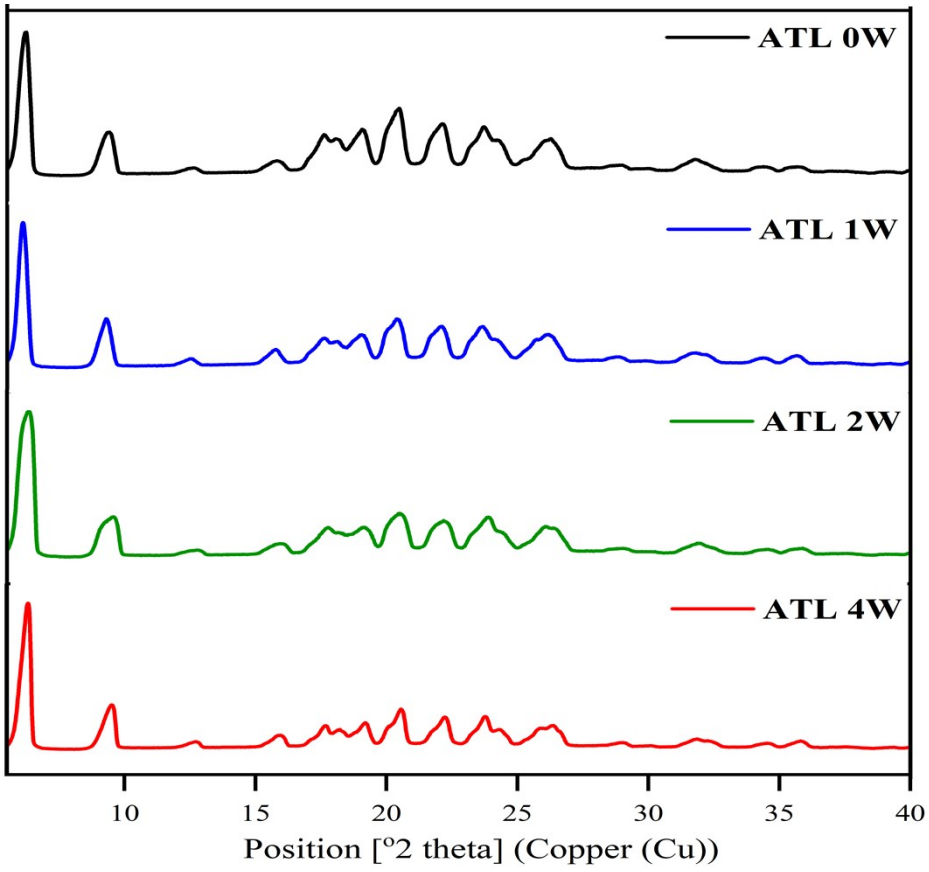
ATL 0W
ATL 1W
ATL 2W
ATL 4W
10
15
20
25
30
35
40
Position [°2 theta] (Copper (Cu))

(a)

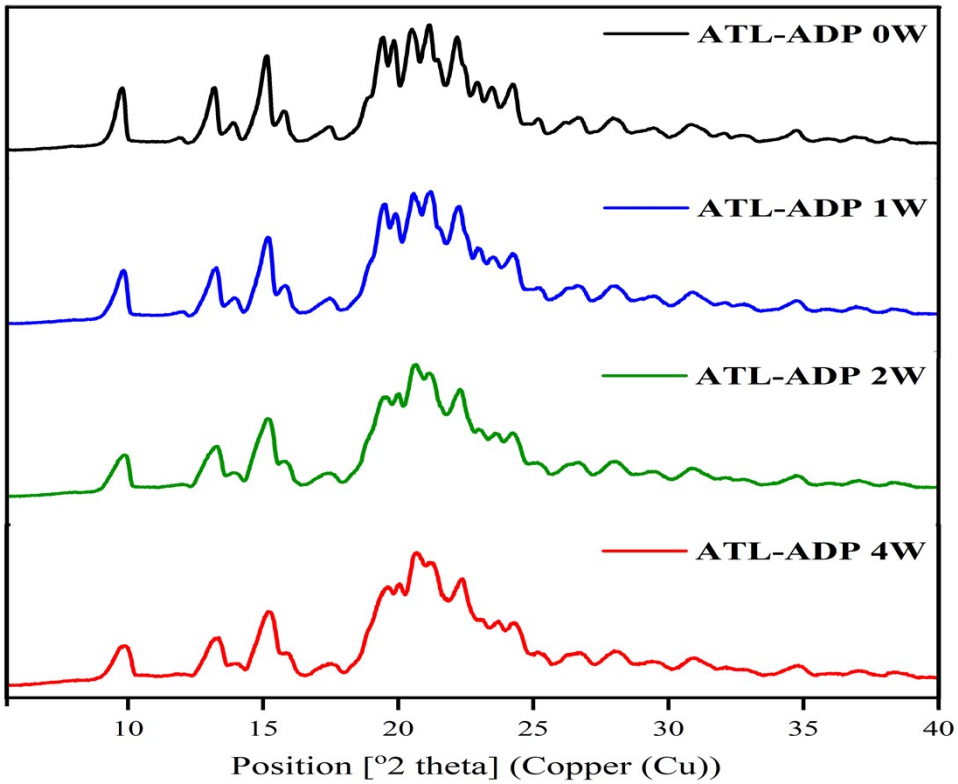
ATL-ADP 0W
ATL-ADP 1W
ATL-ADP 2W
ATL-ADP 4W
10
15
20
25
30
35
40
Position [°2 theta] (Copper (Cu))

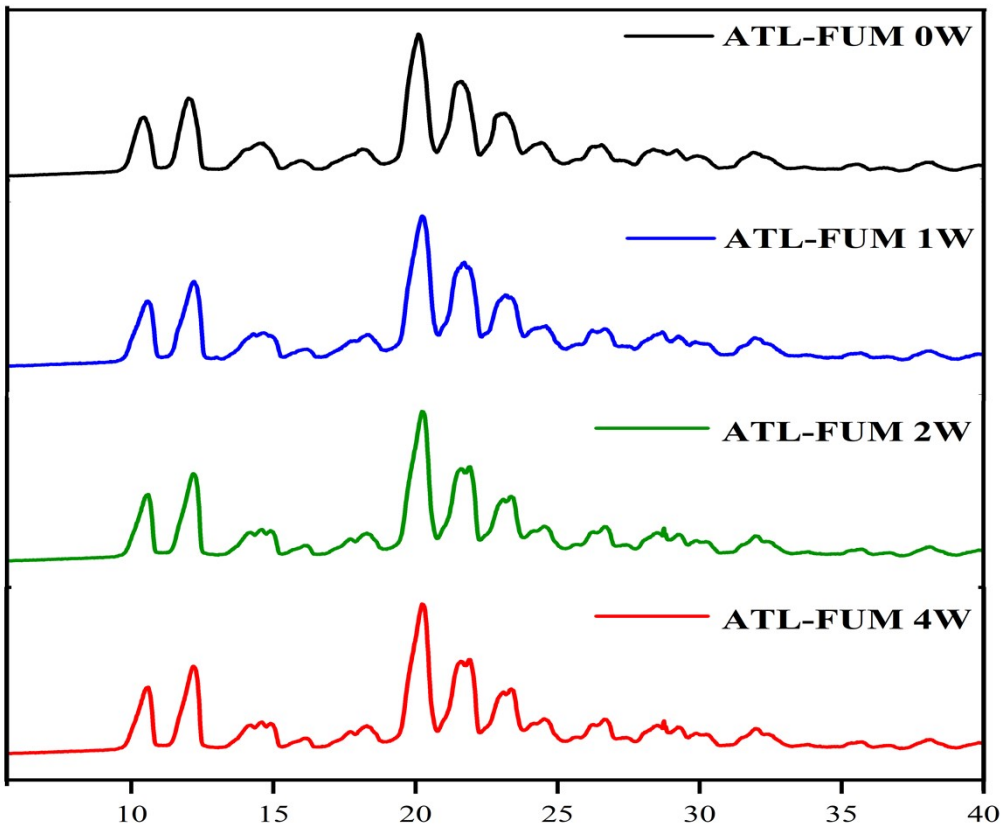
ATL-FUM 0W
ATL-FUM 1W
ATL-FUM 2W
ATL-FUM 4W
10
15
20
25
30
35
40
Position [°2 theta] (Copper (Cu))

(c)

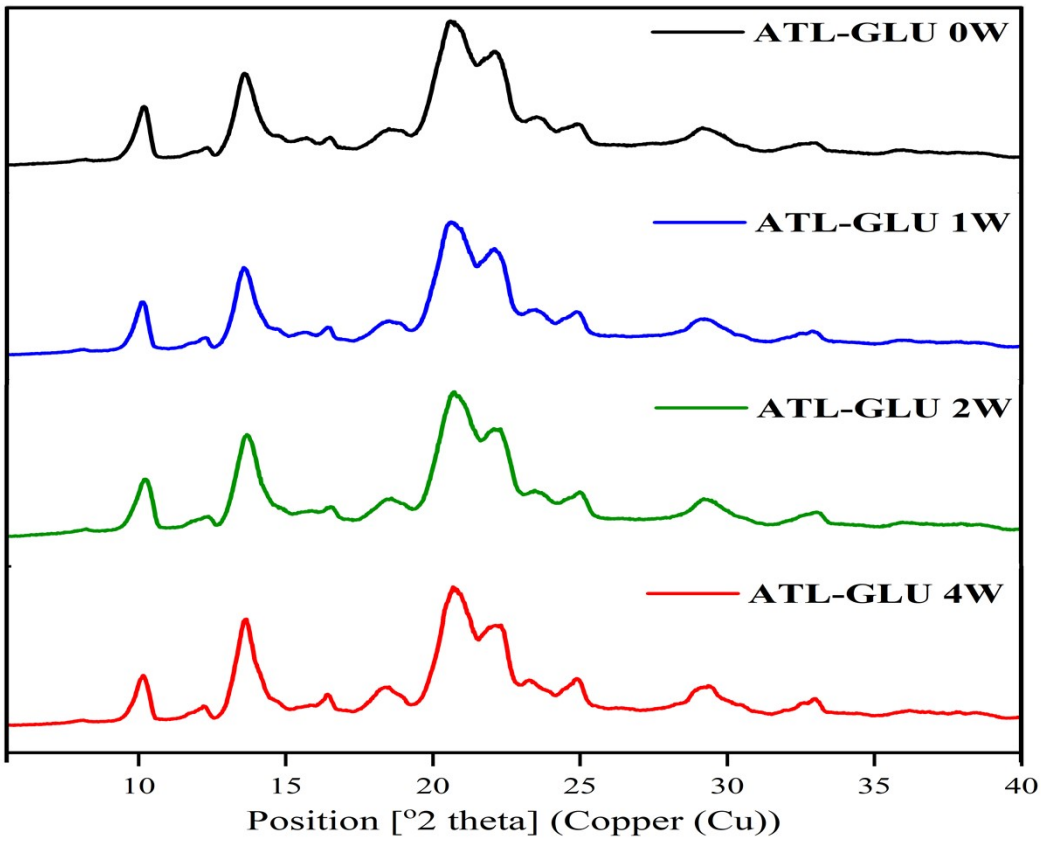
ATL-GLU 0W
ATL-GLU 1W
ATL-GLU 2W
ATL-GLU 4W
10
15
20
25
30
35
40
Position [°2 theta] (Copper (Cu))

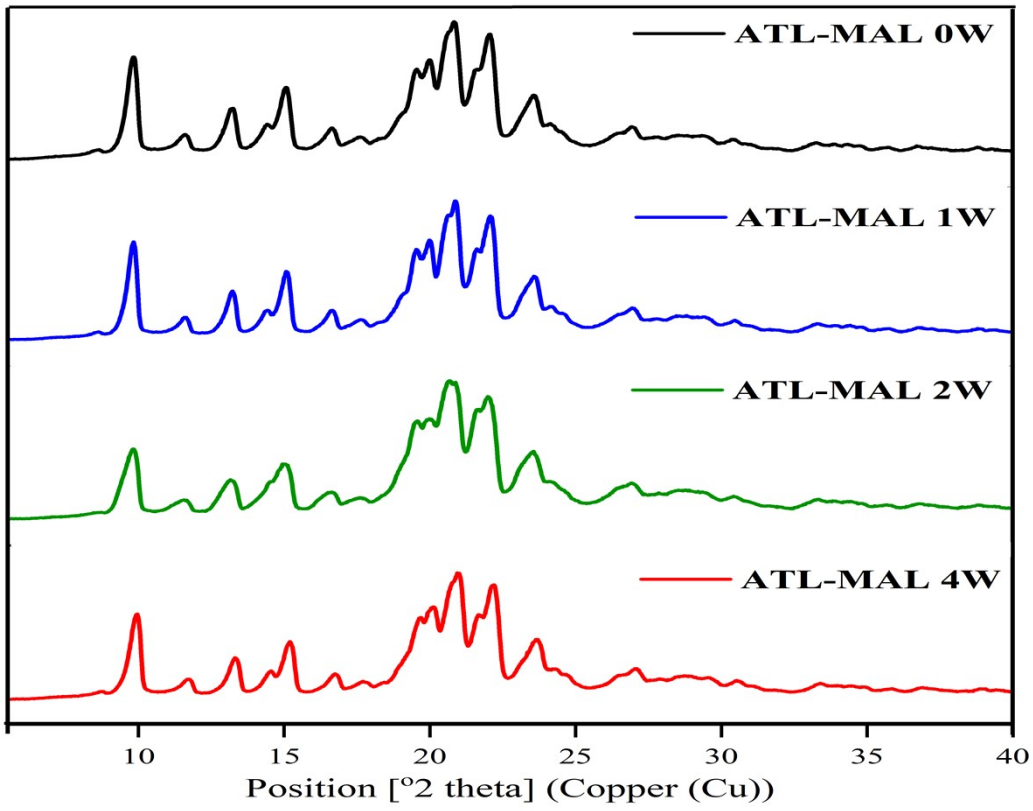
ATL-MAL 0W
ATL-MAL 1W
ATL-MAL 2W
ATL-MAL 4W
10
15
20
25
30
35
40
Position [°2 theta] (Copper (Cu))

(e)

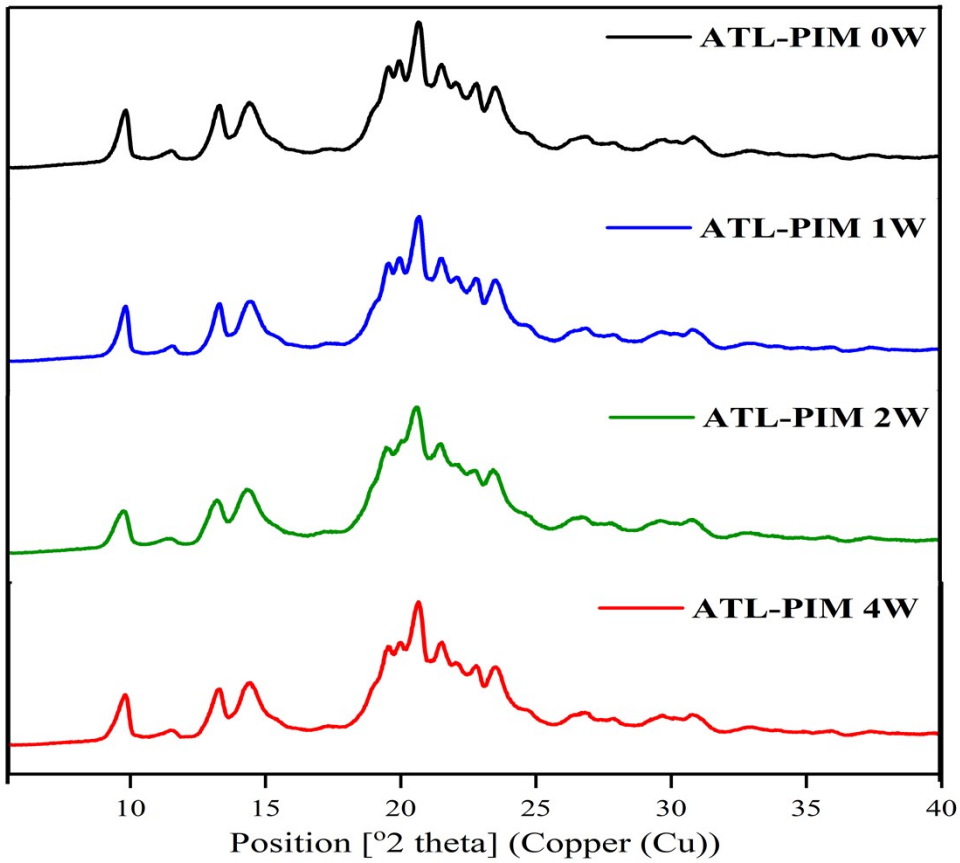
ATL-PIM 0W
ATL-PIM 1W
ATL-PIM 2W
ATL-PIM 4W
10
15
20
25
30
35
40
Position [°2 theta] (Copper (Cu))

(f)

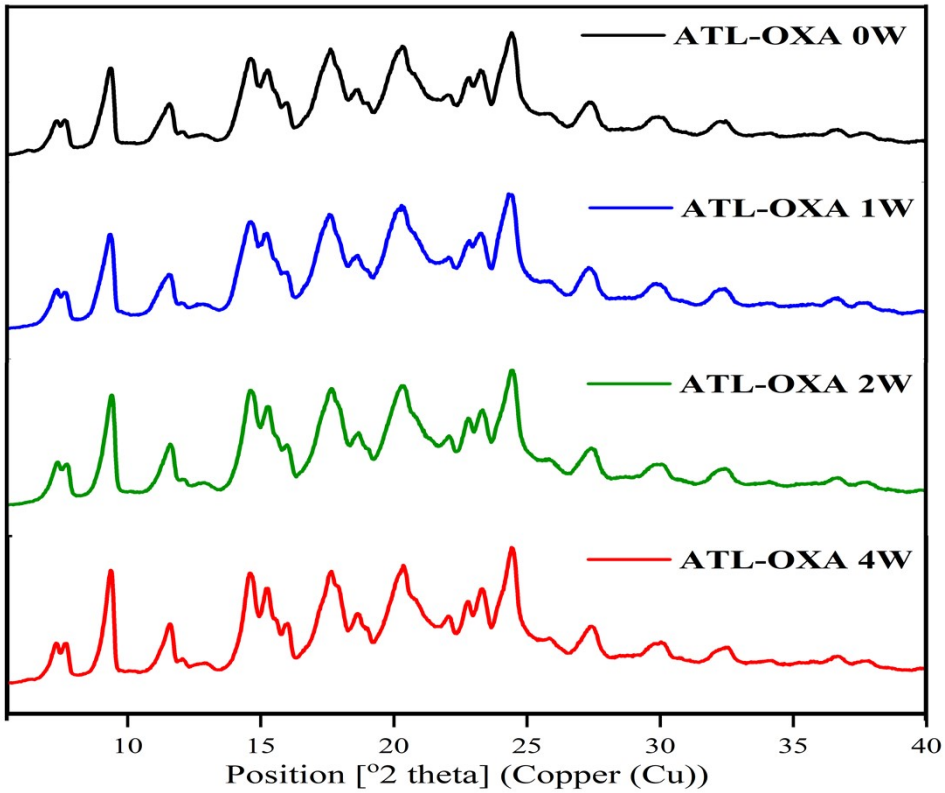

(g)

Figure S8. PXRD comparison of ATL and its salts exposed to 35±5 ^{O}C and 75±5% relative humdity for 4w that confirmed their physical stability (a-g).

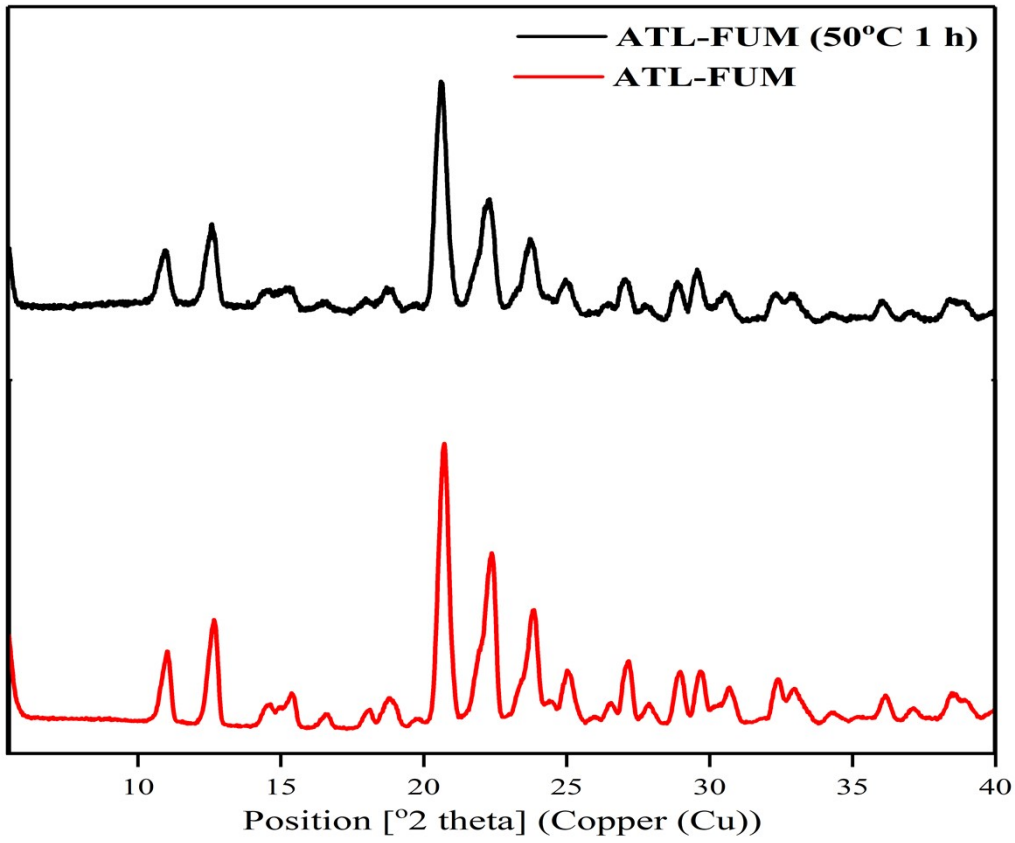

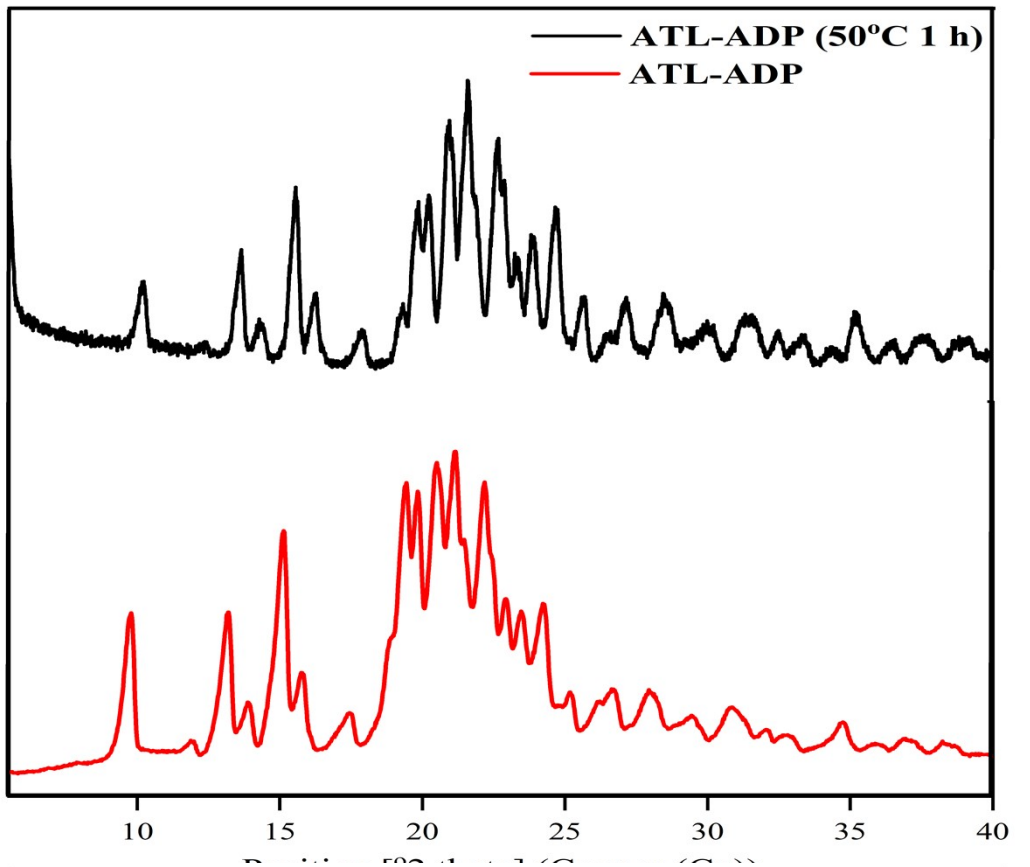
ATL-ADP (50°C 1 h)
ATL-ADP
10
15
20
25
30
35
40

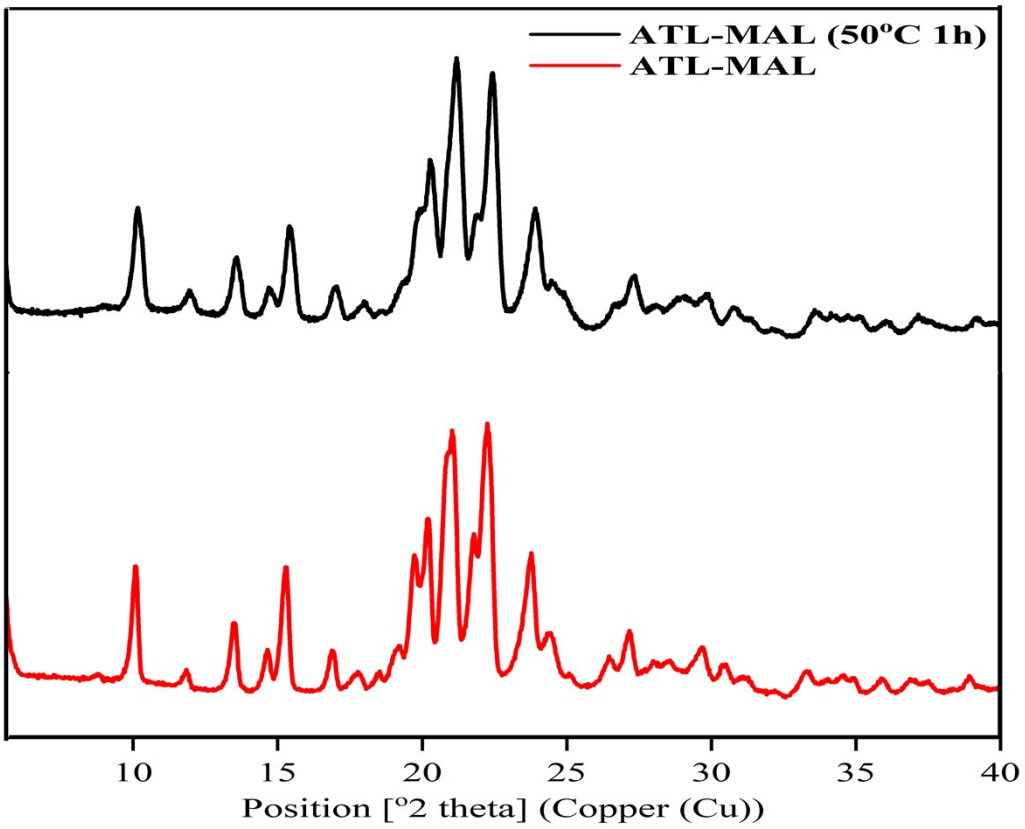
ATL-MAL (50°C 1h)
ATL-MAL
10
15
20
25
30
35
40
Position [°2 theta] (Copper (Cu))

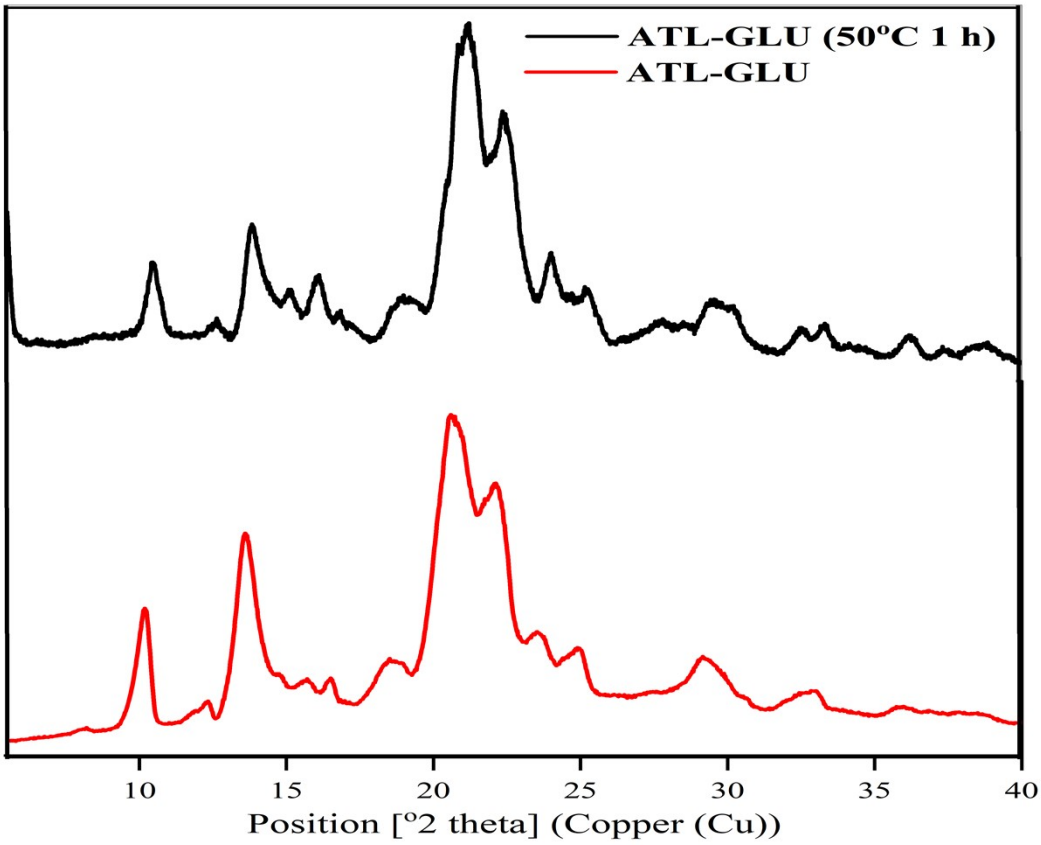
ATL-GLU (50°C 1 h)
ATL-GLU
10
15
20
25
30
35
40
Position [°2 theta] (Copper (Cu))

(d)

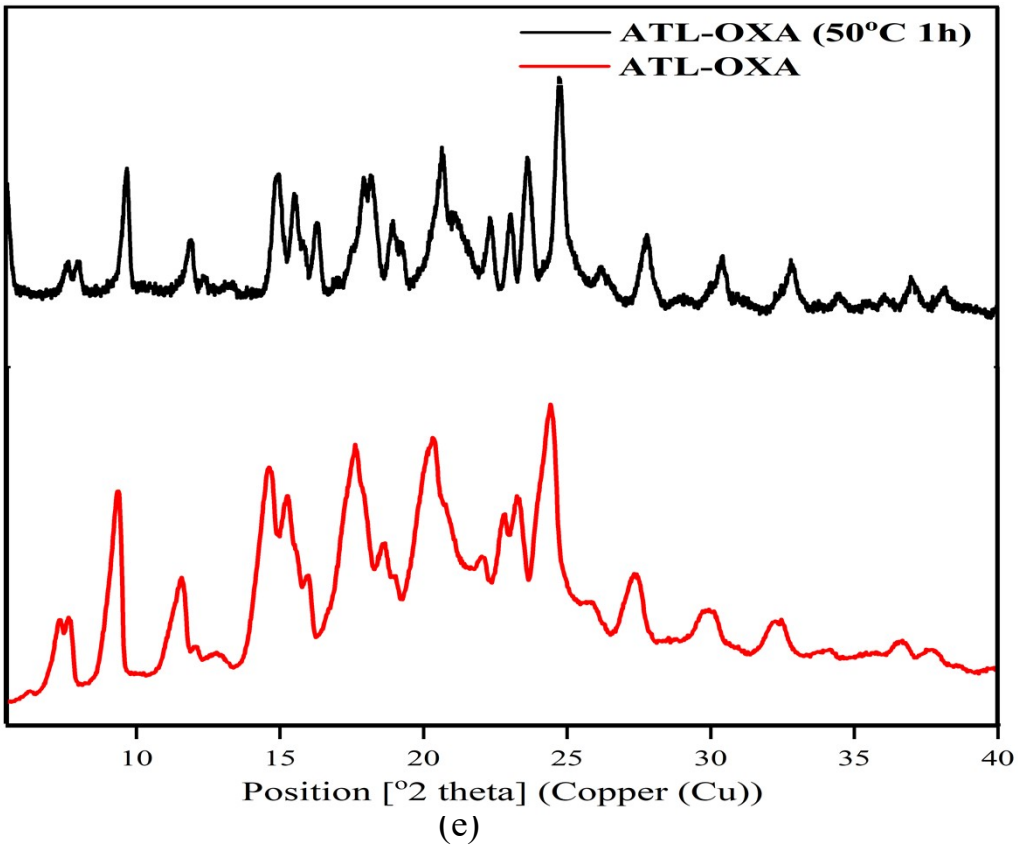
ATL-OXA (50°C 1h)
ATL-OXA
10
15
20
25
30
35
40
Position [°2 theta] (Copper (Cu))

(e)

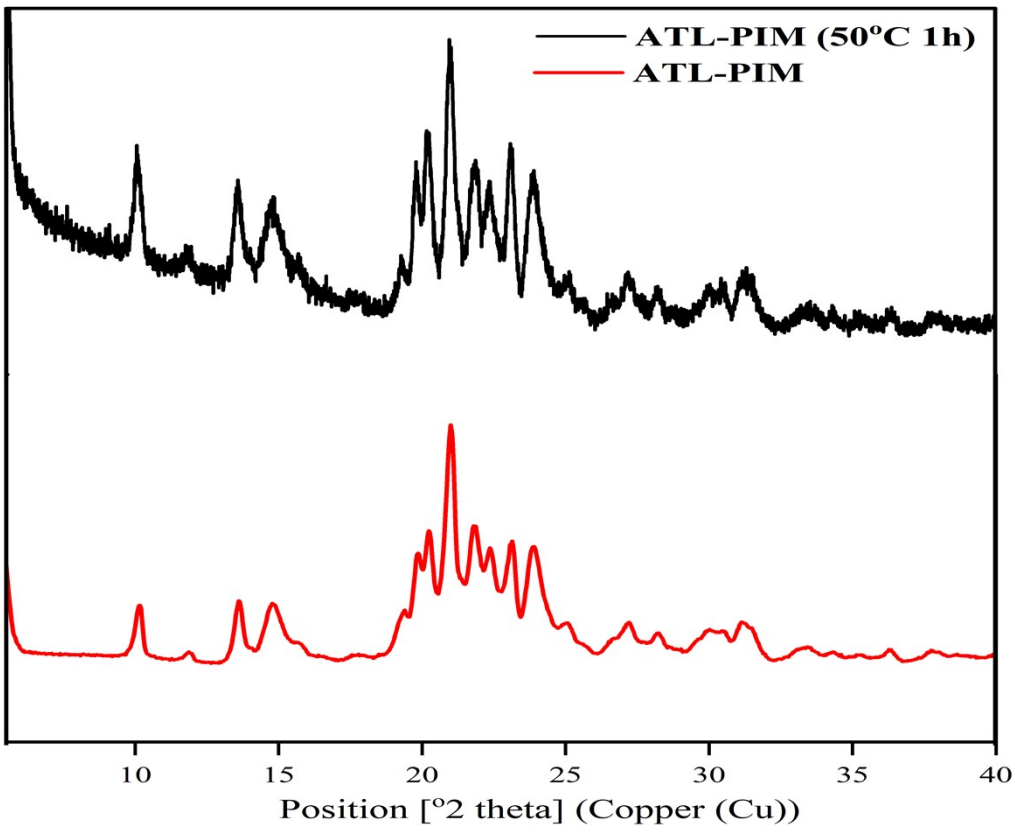

(f)

Figure S9. PXRD comparison of ATL salts at 50 °C for 1h confirms their thermal stability (a-f).